U.S. DEPARTMENT OF ENERGY | Energy Efficiency & Renewable Energy

BUILDING TECHNOLOGIES OFFICE

Internal Roof and Attic Thermal Radiation Control Retrofit Strategies for Cooling-Dominated Climates

A. Fallahi, H. Durschlag, D. Elliott, J. Hartsough, N. Shukla, and J. Kosny
Fraunhofer Center for Sustainable Energy Systems

December 2013

Building America
U.S. Department of Energy

Available electronically at http://www.osti.gov/bridge

Available for a processing fee to U.S. Department of Energy
and its contractors, in paper, from:

U.S. Department of Energy
Office of Scientific and Technical Information
P.O. Box 62
Oak Ridge, TN 37831-0062
phone: 865.576.8401
fax: 865.576.5728
email: mailto:reports@adonis.osti.gov

Available for sale to the public, in paper, from:

U.S. Department of Commerce
National Technical Information Service
5285 Port Royal Road
Springfield, VA 22161
phone: 800.553.6847
fax: 703.605.6900
email: orders@ntis.fedworld.gov
online ordering: http://www.ntis.gov/ordering.htm

Printed on paper containing at least 50% wastepaper, including 20% postconsumer waste

Internal Roof and Attic Thermal Radiation Control Retrofit Strategies for Cooling-Dominated Climates

Prepared for:

The National Renewable Energy Laboratory

On behalf of the U.S. Department of Energy's Building America Program

Office of Energy Efficiency and Renewable Energy

15013 Denver West Parkway

Golden, CO 80401

NREL Contract No. DE-AC36-08GO28308

Prepared by:

A. Fallahi, H. Durschlag, D. Elliott, J. Hartsough, N. Shukla, and J. Kosny

Fraunhofer Center for Sustainable Energy Systems (CSE)

Building Energy Efficiency Group

5 Channel Center Street

Boston, MA 02210

NREL Technical Monitor: Chuck Booten

Prepared under Subcontract No. KNDJ-0-40345-02

December 2013

[This page left blank]

Contents

List of Figures vi
List of Tables viii
Abbreviations ix
Acknowledgment 1
Executive Summary 2
1 Introduction 4
2 Field Testing 8
2.1 Instrumentation 13
2.2 Radiation Control Technology Installations 17
2.2.1 Radiant barrier with enclosed airspace 17
2.2.2 Interior Radiation Control Coating (IRCC) 18
3 Experimental Data Analysis 20
3.1 External and Internal Air Temperature Comparisons 20
3.2 Experimental Attic Air Temperature Comparisons 29
3.3 Experimental Heat Flux Comparison 44
4 Energy Modeling 47
4.1 Model Description 47
4.2 Calibration of Whole Building Energy Model 50
4.3 Prediction of the Cooling Energy Consumption 53
4.4 Modeling Results 53
5 Cost Effectiveness Analysis 56
6 Conclusions 58
References 60
Appendix A- Historical Energy Consumption Data 62

List of Figures

Figure 1. Location of site. 8
Figure 2. Location of thermistor arrays and heat flow transducers inside the tested attics (Right); Bird view image of the duplexes in Austin, TX (Left). 9
Figure 3. Estimated brick wall construction: 2 in. brick, 1 in. air gap, ½ in. OSB, 2×4 stud wall with batt insulation, gypsum wall board (left); Estimated clapboard siding: clapboard, battens, ½ in. OSB, 2×4 stud wall with batt insulation, gypsum wall board (right). 10
Figure 4. Existing insulation conditions in Duplex 1. Note the inconsistent levels of loose-fill insulation. 10
Figure 5. Existing insulation conditions in Duplex 2. Note the inconsistent levels of loose-fill insulation. 11
Figure 6. Existing insulation conditions in Duplex 2 (left) and Duplex 1 attic over living space (above right) and over garage (below right). 12
Figure 7. Visible gaps around ducts entering attic. 12
Figure 8. Location of the vents for attics over living spaces in Duplex 1. 13
Figure 9. Location of the vents for attics over living spaces in Duplex 2. 13
Figure 10. Diagrams of the attic sensor distributions for a RB combined with an enclosed reflective air space (upper diagram), and IRCC and baseline (lower diagram). 15
Figure 11. Thermistors installed on interior, exterior and attic to capture surface temperatures. 16
Figure 12. DAQ Components. 17
Figure 13. Installation of RB with enclosed airspace from Fi-Foil Company (Silver Shield). 18
Figure 14. Installation of IRCC from Solec-Solar Energy Corporation (LO/MIT-II MAX) (left) and from STS Coating, Inc. (HeatBloc-Ultra) (right). 19
Figure 15. Measured exterior air temperature on one of the test houses. 21
Figure 16. Average daily roof surface temperatures recorded during the April measure period. 22
Figure 17. Average daily roof surface temperatures recorded during the June/July measure period. 23
Figure 18. Average daily roof surface temperatures recorded during the July/August measure period. 24
Figure 19. Maximum roof surface temperatures recorded during the April measure period. 25
Figure 20. Maximum roof surface temperatures recorded during the June/July measure period. 26
Figure 21. Maximum roof surface temperatures recorded during the July/August measure period. 27
Figure 22. Average interior air temperatures recorded during the April measure period. 28
Figure 23. Average interior air temperatures recorded during the June/July measure period. 29
Figure 24. Example of attic air temperatures recorded in four test attics (center location) during the April measure period. 30
Figure 25. Average daily attic air temperatures recorded in four test attics (center location) during the April measure period. 31
Figure 26. Average daily attic air temperatures recorded in four test attics (center location) during the June/July measure period. 32
Figure 27. Average daily attic air temperatures recorded in two IRCC attics (center location) during the July/August measure period. 33
Figure 28. Maximum daily attic air temperatures recorded in four test attics (center location) during the April measure period. 34
Figure 29. Maximum daily attic air temperatures recorded in four test attics (center location) during the June/July measure period. 35
Figure 30. Maximum daily attic air temperatures recorded in two IRCC attics (center location) during the July/August measure period. 36
Figure 31. Differences in daily attic air temperatures recorded between three test attics using radiation control technologies and a baseline attic, during the April measure period. 37
Figure 32. Differences in daily attic air temperatures recorded between three test attics using radiation control technologies and a baseline attic, during the June/July measure period. 38
Figure 33. Differences in maximum daily attic air temperatures recorded between three test attics using radiation control technologies and a baseline attic, during the April measure period. 39
Figure 34. Differences in maximum daily attic air temperatures recorded between three test attics

using radiation control technologies and a baseline attic, during the June/July measure period. 40
Figure 35. Daily temperatures on the top surface of the attic insulation recorded in four test attics using radiation control technologies and a conventional base case, during the April measure period. 41
Figure 36. Daily temperatures on the top surface of the attic insulation recorded in three test attics using radiation control technologies and a conventional base case, during the June/July measure period. 42
Figure 37. Daily temperatures on the top surface of the attic insulation recorded in two test attics using radiation control technologies and a conventional base case, during the July/August measure period. 43
Figure 38. Heat fluxes recorded in four test attics using radiation control technologies and a conventional base case, during the April measure period. Positive heat flow direction is from conditioned space to the attic. 44
Figure 39. Heat fluxes recorded in test attics using radiation control technologies and a conventional base case, during the June/July measure period. Positive heat flow direction is from conditioned space to the attic. 45
Figure 40. Heat fluxes recorded in test attics using radiation control technologies and a conventional base case, during the July/August measure period. Positive heat flow direction is from conditioned space to the attic. 46
Figure 41. Duplex 1 model (above); Duplex 2 model (below). 48
Figure 42. Breakdown of household gas consumption. 50
Figure 43. Comparison of monthly historical gas bill, simulated consumption, and the gas consumption by Texas Gas Service calculator. The calibration is limited to the months with available historical utility bill. 51
Figure 44..Breakdown of household electrical consumption. 52
Figure 45. Comparison of monthly historical electricity bill, simulated consumption, and the electricity consumption by Texas Gas Service calculator. The calibration is limited to the months with available historical utility bill. 53
Figure 46. Modeled utility consumption of baseline house in different U.S. South climates and payback period of radiation control strategies. 56

Unless otherwise noted, all figures were created by the Fraunhofer team.

List of Tables

Table 1. Experimental Results for Cooling Load and Heat Flux Reductions Produced by Application of RB 6
Table 2. Model parameters 49
Table 3. Predicted Energy Saving From RB Technology 54
Table 4: Residential utility price based on considered climates 57

Unless otherwise noted, all figures were created by the Fraunhofer team.

Abbreviations

DAQ	Data Acquisition
IRCC	Internal Radiation Control Coating
OSB	Oriented Strand Board
RB	Radiant Barrier

Acknowledgment

We would like to acknowledge and extend our sincerest thanks to the City of Austin, Texas, and Foundation Community for collaborating and providing us with the test houses, Tim Ashwood from Fi-Foil Company, Robert Aresty from SOLEC-Solar Energy Corporation and John Kovacs from STS Coatings for providing and installing the two radiation control technologies, Dr. David Yarbrough from R&D Services, Inc. (RIMA liason), and Dr. Mario Medina from the University of Kansas for assistance and technical guidance.

Executive Summary

This project evaluates the cooling energy savings and cost effectiveness of radiation control retrofit strategies for residential attics in U.S. cooling-dominated climates. Usually, in residential applications, radiation control retrofit strategies are applied below the roof deck or on top of the attic floor insulation. They offer an alternative option to the addition of conventional bulk insulation such as fiberglass or cellulose insulation. Radiation control is a potentially low-cost energy efficiency retrofit strategy that does not require significant changes to existing homes. In this project, two groups of low-cost radiation control strategies were evaluated for southern U.S. applications. One uses a radiant barrier composed of two aluminum foils combined with an enclosed reflective air space and the second uses spray-applied interior radiation control coatings (IRCC).

The main goal of this study, conducted by the U.S. Department of Energy (DOE) Building America team, Fraunhofer Center for Sustainable Energy Systems (Fraunhofer CSE), was to answer the following three research questions:

- What are the potential reductions in annual cooling energy consumption and cooling loads from using a Radiant Barrier (RB) assembly that includes an enclosed reflective air space in residential attics?
- What is the energy performance of an attic-applied IRCC?
- What are the cost benefits of these radiation control technologies in residential retrofit applications located in the southern climate zone?

Both experimental and numerical analyses were used to answer these research questions. Working with the City of Austin, Texas, and Foundation Communities, test houses were selected to apply IRCC and RB systems for field testing and performance analysis. During the 2012 cooling season, thermal performance measurements were completed on four housing units in two residential duplexes. One test attic was retrofitted using RBs and two were retrofitted using IRCCs. The fourth unmodified attic was used as a base case for comparisons. All test houses were occupied during the testing. The plan was to keep internal load schedules in the test units as close as possible.

In general, measured test data confirmed prior results from other research organizations. A 3.4°C reduction of the average attic air temperature was observed for the multifoil RB (two reflective layer of ε=0.03 and ε=0.04) during mid-summer 2012. The recorded data showed a 34% reduction of the attic-generated cooling loads. The potential whole building cooling energy savings for this technology may be close to 4% (assuming approximate steady-state heat transfer, an average attic temperature of 35°C, and internal air temperature of 25°C). This is based on the report that in U.S. residential houses, roofs and attics generate an average 12% cooling energy contributions. In that light, potential whole building cooling energy savings may reach about 4% depending on other building parameters and HVAC system efficiency.

A 2.4°C reduction of the average attic air temperature was observed for the IRCC test sites. This can be equivalent to a 24% reduction of the attic-generated cooling loads and the potential whole building cooling energy savings for this technology may be close to 3%. Based on the recorded

data, the energy performance of two IRCC systems with emissivity of 0.17 and 0.19 seems to be very similar (there were minor differences in construction). To better characterize these technologies, more precise calorimetric field experiments should be considered in the future.

An EnergyPlus computer model calibrated against both pre-retrofit and post-retrofit energy consumption data was used to predict the potential cooling energy savings. The results from EnergyPlus were well below the range of observed cooling energy savings approximated on the measurements performed during this experiment. The modeled whole-building cooling energy savings was 1.3% and 0.8% for RB and IRCC respectively (compared with 4% and 3% during this experiment). The discrepancies could be partially due to EnergyPlus limitation that uses simplified numerical algorithm for attic thermal analysis.

To evaluate the payback period, the heating and cooling loads were modeled for the baseline house with R-19 attic insulation using EnergyPlus in four southern U.S. locations. Having these modeled loads, one upper limit and one lower limit for the radiation control strategies load savings were assumed. The upper limit was obtained from the literature and the lower limit has cooling energy savings close to this report’s field study data. Taking the upper limit of energy savings, RB and IRCC systems yielded the shortest payback times for Miami, Florida and Phoenix, Arizona—about 3.5 years and 5 years, respectively. When saving levels are similar to recorded levels during this experiment (lower limit saving), the payback times are 16 and 22 years, for RBs and IRCC, respectively, for the same locations.

1 Introduction

According to the Reflective Insulation Manufacturers Association (RIMA)[1], radiation control techniques can be grouped in three main product types: a) reflective insulations; b) radiant barriers (RB); and c) Interior Radiation Control Coatings (IRCC). Each of these product types is represented in ASTM Committee C 16 and have standards in print. The "insulation" market share for all products is estimated to be between 1% and 2%. This report will focus on the use of RB and low-emittance (low-e) coatings. In this project, the Fraunhofer team worked closely with RIMA and three companies Fi-Foil, Solec, and STS Coatings, Inc..Interaction between RIMA and Fraunhofer CSE was supported by R&D Services—simultaneously a member of the Building America team led by Fraunhofer CSE and technical advisor to RIMA.

In this report, the physical principles that make RBs and IRCCs work are explained; their thermal performance is discussed based on results of numerical analysis and full-scale field testing.

Attic RBs and IRCCs present a unique way of increasing the thermal performance of existing or new insulation within the space between the roof deck and ceiling level in residential and small commercial buildings. These systems may also be successfully applied in the space between roofs and suspended ceilings in commercial buildings. Attic RBs save energy by reducing the transfer of heat from the hot roof to the attic floor insulation in the summer. The transfer of heat from the attic floor insulation to the roof in the winter is also reduced. Aluminum surfaces, like those found in RB applications, have thermal emittances in the range of 0.03 to 0.06. Therefore, there is very little radiant transfer across a space bounded by a RB.

Most often, RBs are aluminum foil laminates or aluminized synthetic films sheets. The foils are laminated to paper, most commonly to Kraft paper, synthetic films, oriented strand board (OSB), or plywood. For the aluminized synthetic films, a thin layer of aluminum particles are deposited on the films through a vacuum process. These laminates and films are characterized by having at least one low-e surface of 0.1 or less (ASTM C 1313, 2010).

IRCCs are low-e coatings or paints that, when applied (i.e., sprayed or painted) to building surface (e.g., OSB, plywood, metal siding, or plasterboard), decrease the emittance of these surfaces to 0.25 or less (ASTM C 1321, 2009). Both RBs and IRCCs have received considerable attention due to their potential to reduce the radiant heat transfer across vented spaces between roofs and ceilings of buildings (e.g., attic spaces in residential buildings). In the case of RBs, aluminum is used because it is inexpensive and is a surface that, once exposed to air, becomes covered with a layer of a transparent oxide that protects it from the atmosphere and allows it to maintain a constant emittance for long periods of time (Lenntech, 2010).

[1] The Reflective Insulation Manufacturers Association-International (RIMA-I) is a trade association organized to support and encourage the use of reflective technology to conserve energy use in buildings. The Association has 25 members of which 20 are from the United States and 5 are international. Approximately 20 of the members would be considered small businesses. (Dupont, Louisiana Pacific, Sealed Air, Pactiv and Roy-o-Martin are not small businesses.)

In some cases, an RB can include an enclosed air space in order to provide thermal resistance to the path between the roof sheathing and the attic floor. This project uses an RB with an enclosed air space, which is a common configuration with multilayer products such as Silver Shield from Fi-Foil Company. In some cases, there is an R-value [2] [3] associated with the reflective insulation component application. In the configuration considered in this research, the thermal performance of interior-facing RB has to be combined with the low thermal conductive performance of the enclosed air cavities.

Low-e coatings (IRCCs) have similar heat reduction principles as RBs in residential attics. RB coatings are also being studied in this project at Austin, Texas. This is a crucial project for the industry since there are very few examples of directly measured savings due to spray-applied or liquid-applied attic IRCCs.

A recently completed review of prior research on RBs (Medina, 2012) indicates a reduction in summer ceiling heat loads between 23% and 45%. Winter heat load reductions were equal to approximately 40% of the summer reduction. Although the industry does not have software to evaluate energy savings, there is an ASTM Consensus method for calculating RB performance (ASTM C 1340, "Standard Practice for Estimation of Heat Gain or Loss through Ceilings Under Attics Containing Radiant Barriers by Use of a Computer Program"). This program is called "AtticSim" and was developed by Kenneth Wilkes. In the past, it has been used by Oak Ridge National Laboratory to generate input for two editions of DOE RB fact sheets.

Currently, RBs and IRCCs are difficult to numerically analyze using whole building energy simulation tools. In the past, DOE 2.2, EnergyPlus, and BEopt have not had the capability for detailed attic modeling. Recently, there has been an effort to link C 1340 to DOE 2.2 and provide modeling of attic RBs. However, the status of this project is unclear. Current DOE-sponsored work with AtticSim is limited to attic RBs and does not extend to evaluations of reflective insulation assemblies. Additionally, Fraunhofer CSE used AtticSim to analyze the thermal performance of complex attic configurations. The organizations listed above have utilized AtticSim in their research because it is an in-house program that has the recognition of being a consensus program.

Medina (2012) reviewed over sixty published papers from various sources. These included peer-reviewed journals, peer-reviewed conference proceedings, national and state laboratory reports, MS theses, and Ph.D. dissertations. Based on the report, experimental results highlighting cooling load and ceiling heat flux reductions produced by RBs vary depending on nominal ceiling insulation R-value, testing protocol, climate zone, ventilation type, occupancy and duct inclusion in the attics. Medina (2012) reported that in attics with nominal insulation levels of R-11, R-19 and R-30, average space cooling reductions are 14%, 20% and 6%, respectively. He also reported the average reduction in heat flow produced by installing RBs in attics with

---

[2] Thermal resistances calculated for an enclosed air space with one surface having emittance 0.03 and a second surface with emittance 0.9 are 1.99 and 3.43 (ft2•h•°F/Btu) when heat directions are up at 45° and down at 45°, respectively. The thermal resistance values in the report do not include the effect of the air space between the product and the roof sheathing of the RB effect due to a low-emittance surface facing the attic floor.

[3] http://www.rimainternational.org/index.php/technical/library/residential-commercial/ .

insulation levels of R-11, R-19 and R-30 are 45%, 30% and 23%. The aforementioned savings are listed in below in Table 1.

According to Medina (2012), laboratory-controlled experiments of IRCC applied in a flat system configuration with an insulation level of R-19, produced average heat flow reductions of 32% (vs. the same system without the application of any coatings).

Table 1. Experimental Results for Cooling Load and Heat Flux Reductions Produced by Application of RB.

	Nominal Insulation Level (R-value)	Saving Range (%)	Average Saving (%)
Cooling Load Reduction	R-11	11-16	14
	R-19	13-27	20
	R-30	Below 16[4]	6
Ceiling Heat Flux Reduction	R-11	34-60	45
	R-19	16-43	30
	R-30	20-25	23

In this project, Fraunhofer CSE worked with a team of local companies in order to field test three radiation control technologies:

1. In collaboration with RIMA, Foundation Communities and City of Austin, the three following building enclosure technologies were installed in test houses in the Austin project in September 2011:
    a. Two low-cost IRCC, a non-thickness dependent, low-e coating. IRCCs are usually applied by spray to roof deck boards.
    b. RB integrated with sheathing material and air cavity; in this project; two layers of aluminum and an enclosed air space.

2. Test instrumentation (necessary to install during the retrofit process) was installed in two duplex houses that were selected for the field testing (each half of the duplex represented a separate housing unit). Attics between separate units (two tenants per duplex) were thermally divided and insulated. The following test configuration was installed:
    a. First duplex: IRCC coating and baseline attic
    b. Second duplex: IRCC coating system and RB system.

3. Cost data from installation of the tested radiation-control technologies were collected.

These systems were installed in two duplexes in Austin. One unit, where none of the radiation control technologies were installed, established the baseline. The other three units underwent modifications to incorporate the systems described above, taking care to minimize alterations to existing conditions so that a direct comparison could be done post-retrofit. All units had heat flux transducers and thermistors installed to monitor both surface and air temperatures.

[4] Based on Medina, 2010, when the attic insulation levels were R-30, the range of space cooling load reductions produced by the RBs ranged from -1% to 16%. The -1% indicates that there was one case in which the reported space cooling load once the RBs was installed was higher than before the RB was installed.

Comparisons of attic air temperatures were made to assess system performance. Although heat flux is an indicator of the heating or cooling loads, air temperature reflects the unique conditions of each unit as well as the loads. These unique conditions included varying parameters within the four units that could not be changed or controlled. Notable variations between the four cases include:

- *Ventilation of conditioned space* – Occupants operating windows and adjusting HVAC systems varied the flow rate greatly
- *Air leakage through ceiling* – Craftsmanship of ceiling construction varied by apartment (i.e. holes around pipes, ducts, etc.)
- *R-value of attic* – Construction and insulation type and thickness varied between duplexes
- *Internal temperatures* – Occupants adjusted the thermostat causing non-uniform temperatures between units.

Finally, representative computer models were constructed to further enhance understanding of the radiation control systems. Comparisons to the utility consumption data were made from the simulation results.

2 Field Testing

The test houses consisted of two duplex houses in Austin, which were closely located to each other (< 0.1 miles apart, see Figure 1 and Figure 2). The duplexes were both constructed of 2×4 wood framing with brick or wood cladding. Figure 3 shows best estimates of the wall composition. Duplex 1 was built between 1987 and 1997 and Duplex 2 was a pre-1987 construction. Each duplex has two attached, unconditioned garages. The windows were operable, single glazed in non-thermally-broken aluminum frames.

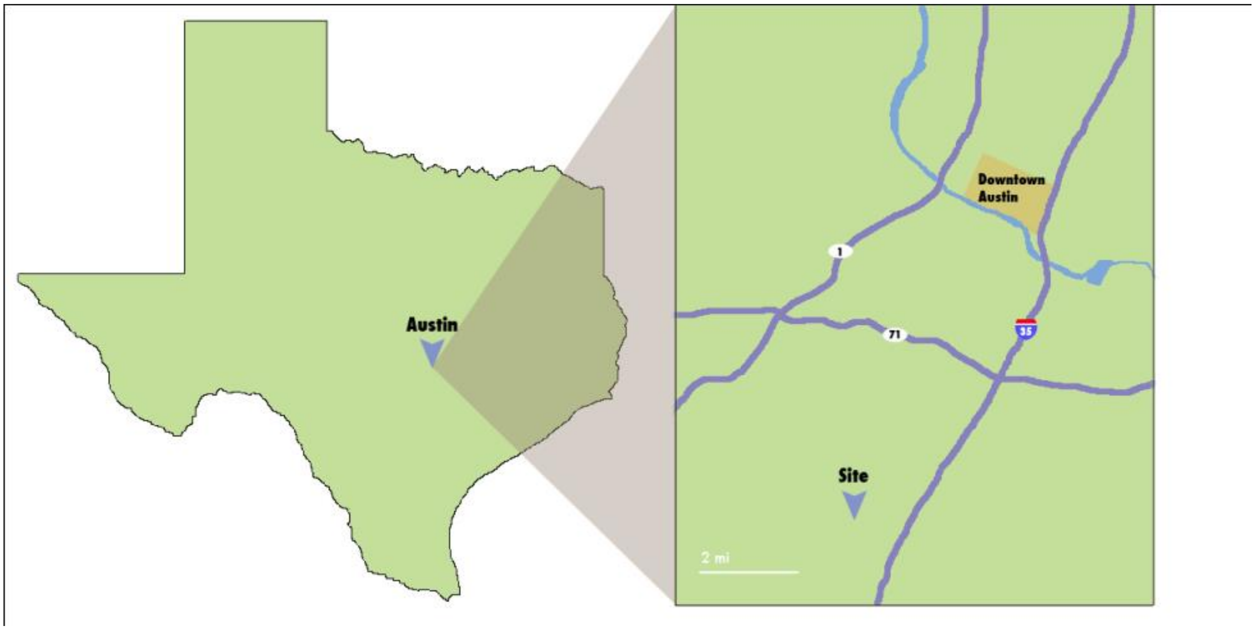

Figure 1. Location of site.

The attics over the garages are separated from the attics over the houses and were not installed with the radiant control technologies. In order to thermally separate the test units, the attics over the houses were divided by insulated walls for the purpose of this field study. The ceilings were flat in Duplex 1 and vaulted in Duplex 2. Overall, the insulation was very non-uniform in all test attics. In several places, the loose-fill cellulose could reach depths such that the R-values equal approximately R-30 but were lower at other places. Duplex 1 had loose-fill cellulose and loose-fill fiberglass near the garage and Duplex 2 had a layer of batt insulation with loose cellulose on top. Four different test cases (see Figure 2) were established:

1. Duplex 1
    A. Nothing added to the east attic (used as baseline)
    B. IRCC (LO/MIT) added to the west attic
2. Duplex 2
    A. RB added to the east attic
    B. IRCC (HeatBloc-Ultra) added to the west attic.

Unfortunately, there was no opportunity to measure the performance of the four units prior to the retrofits in order to establish a baseline in each unit without radiation control technologies. There was an option to make the aforementioned insulation levels consistent; however, this would have made the utility bill calibration comparison impossible. For this reason, it was decided to maintain post-retrofit conditions, such as infiltration and insulation, as closely as possible to the pre-retrofit conditions. The only exception to this was the addition of rigid polyisocyanurate insulation in the attic as a divider to thermally separate the two units. Considering the attic air temperature difference created by applying these technologies is small, the applied insulating divider isolates the effect of each technology from each other.

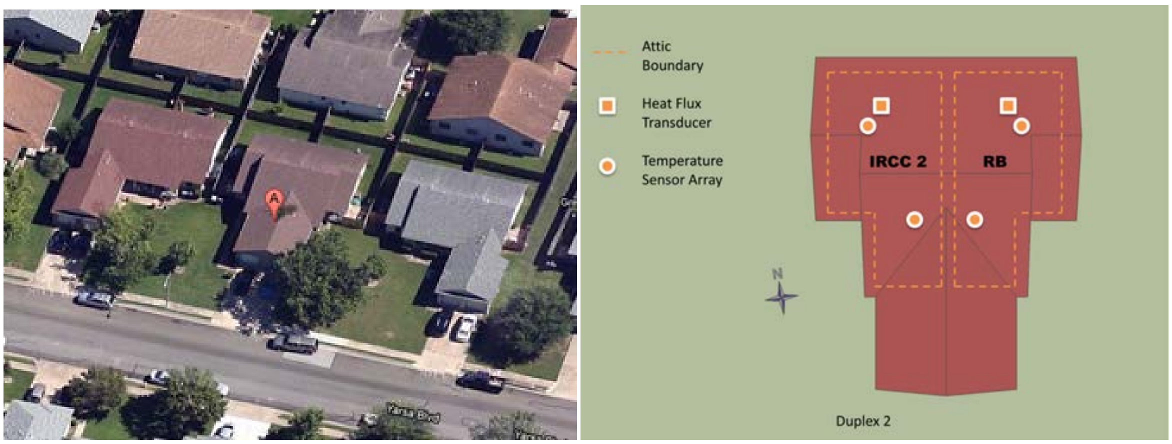

Source: maps.google.com

Duplex 2

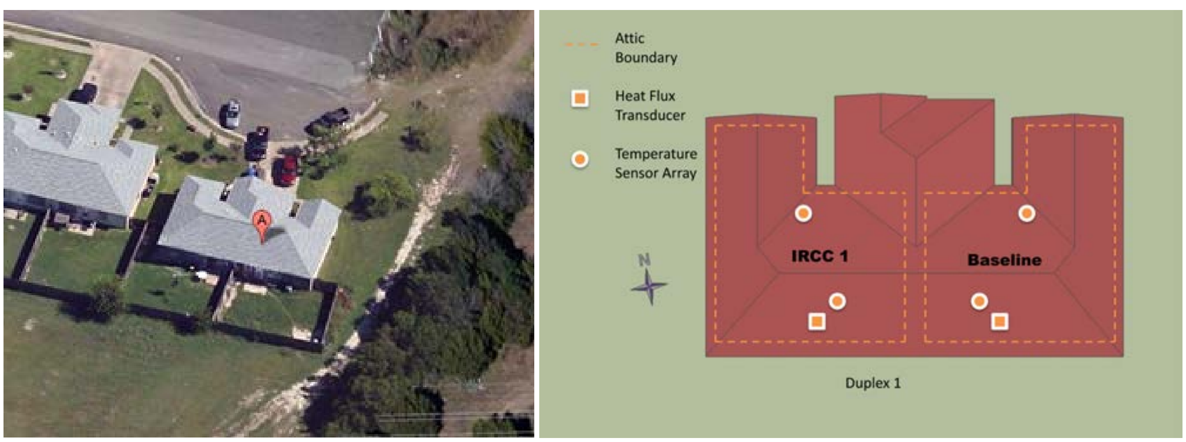

Source: maps.google.com

Duplex 1

Figure 2. Location of thermistor arrays and heat flow transducers inside the tested attics (right); Bird view image of the duplexes in Austin, TX (left).

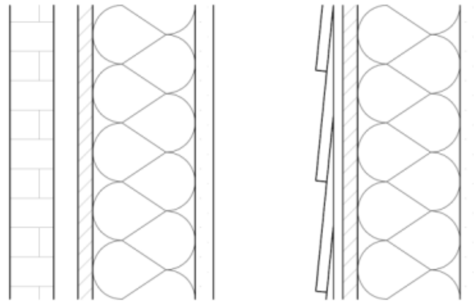

Figure 3. Estimated brick wall construction: 2 in. brick, 1 in. air gap, ½ in. OSB, 2×4 stud wall with batt insulation, gypsum wall board (left); Estimated clapboard siding: clapboard, battens, ½ in. OSB, 2×4 stud wall with batt insulation, gypsum wall board (right).

Duplex 1 consisted mainly of loose-fill cellulose insulation. It was blown between and leveled with 2×8 joists. The cellulose distribution was more even than in the other duplex. However, the areas above and close to the garage were blown with loose-fill fiberglass insulation on top of cellulose. The fiberglass thickness varied from less than 1 in. to over 10 in. above garage area.

Figure 4. Existing insulation conditions in Duplex 1. Note the inconsistent levels of loose-fill insulation.

Duplex 2 had a vaulted ceiling and had two layers of insulation in the attic. The first layer is fiberglass batt installed between and leveled with 2×4 joists and the second layer on top is loose fill cellulose insulation. However, the loose fill cellulose is not evenly distributed; at some locations there is close to 1 in. cellulose insulation in the middle of the attic and over 6 in. along the eaves.

Figure 5. Existing insulation conditions in Duplex 2. Note the inconsistent levels of loose-fill insulation.

When field testing began, there was an option to evenly distribute the insulation; however, this would change the thermal condition of the attics and would make it difficult to use a historical utility bill for comparison and calibration of the EnergyPlus models.

Poor craftsmanship was evident in the partition between the attic and spaces below. Large holes were noticed in the plywood where ducts entered from the HVAC closet in Duplex 2, shown in Figure 7. This allowed air to flow from the garage, where the utility closet was located, to the attic. Measured air leakage values were also quite high in the living space due to the uninsulated, unsealed door linking the garage and kitchen. Therefore, the garage was unintentionally semi-conditioned. Ventilation in the attic over the living spaces in Duplex 1 is through soffit vents and ridge vents (Figure 8). The venting area is approximately 15.5 ft^2 (approximately equivalent to 1:50 ventilation rate). Duplex 2 has sparsely distributed soffit vents and gable end vents (Figure 9). The venting area is approximately 12 ft^2 and the ventilation rate is estimated to be 1:75.

A blower door test was attempted in the living space, indicating air changes per hour to be between 4 and 7 ACH. However, the confidence in these results was low since there was great difficulty in pressurizing the houses. This was due to the air leakage between the living space and the garage.

Historical utility data of the houses for existing condition configurations were collected and used for energy performance comparisons of each individual attic, as well as calibration of the computer energy model discussed in Chapter 4.

Existing insulation in Duplex 2 attic

Existing conditions in Duplex 1 attic over the garage

Existing conditions in Duplex 1 attic over the garage

Figure 6. Existing insulation conditions in Duplex 2 (left) and Duplex 1 attic over living space (above right) and over garage (below right).

Figure 7. Visible gaps around ducts entering attic.

Figure 8. Location of the vents for attics over living spaces in Duplex 1.

Figure 9. Location of the vents for attics over living spaces in Duplex 2.

2.1 Instrumentation

Each partitioned attic has been instrumented to measure thermal energy flows and included thermistor arrays for the test attics and heat flux transducers on the ceiling between the living zone and the attic zone. In addition, a weather station was installed to measure outdoor climatic parameters. The attic instrumentation diagram is illustrated in Figure 10 for the two different installed technologies.

Unit 2A

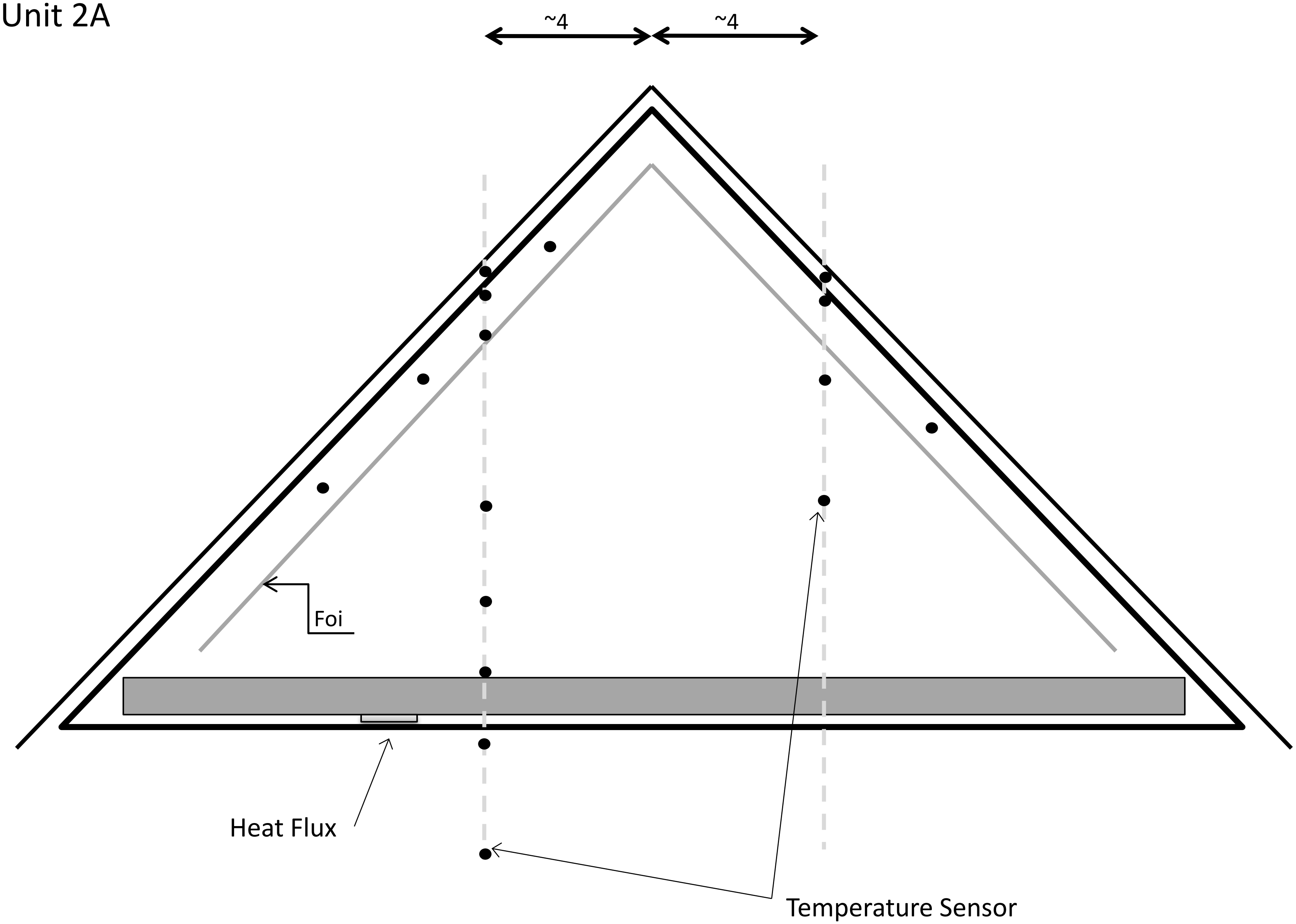

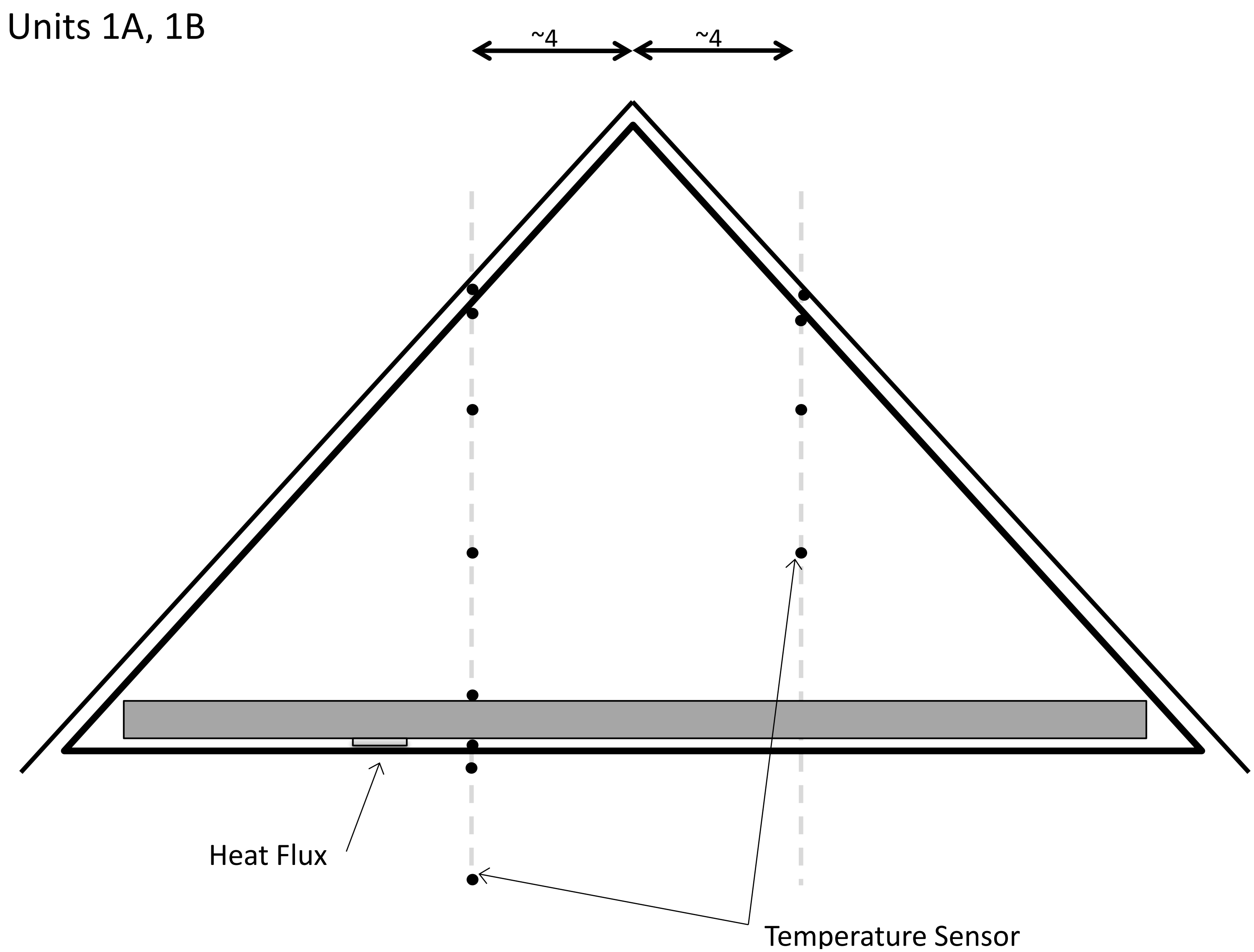

Figure 10. Diagrams of the attic sensor distributions for a RB combined with an enclosed reflective air space (upper diagram), and IRCC and baseline (lower diagram).

The team measured temperatures using shielded thermistors. Two arrays of thermistors were installed at each attic: one on the underside of the south-facing roof and the other under the north-facing roof. To measure surface temperatures, thermistors were bonded to surfaces using epoxy resin (see Figure 11).

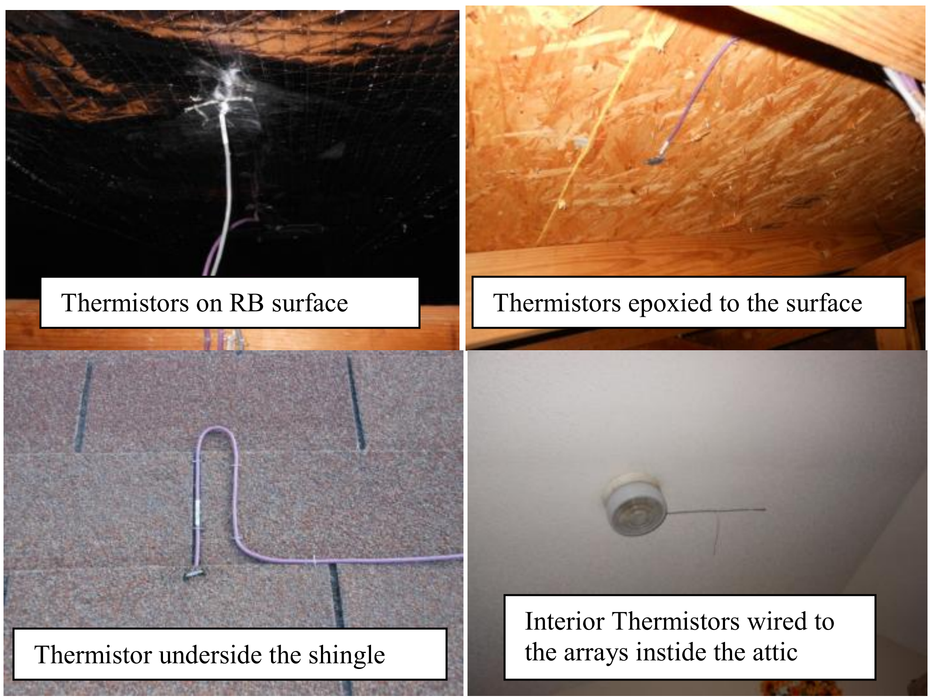

Figure 11. Thermistors installed on interior, exterior and attic to capture surface temperatures.

Heat flux transducers measured the energy flow through the attic floors. Each attic transducer was first installed on a 1 ft×1 ft gypsum board panel and then placed on the ceiling gypsum board. To keep a flat contact surface between two gypsum boards without any air gap, shallow grooves were cut into the 1 ft×1 ft gypsum panels to place the heat flow transducer and the wires, and then secured with epoxy. This method allowed good contact without damaging interior finishes of the building. The location of the heat flow transducers was close to the thermistor array as shown in Figure 10. Pictures of these technologies in-situ can be found in Figure 11.

The temperature sensors used for this experiment were 10K Ohm thermistors. The thermistor sensors were acquired as leaded elements that were soldered to lengths of shielded twisted-pair, two-conductor cables, and the tips were encapsulated with thermally conductive epoxy (Resinlab EP1200). The completed assembly was then calibrated using a Fluke 9171 Metrology Well and a Keithley 2700 Digital MultiMeter through seven temperature points.

The heat flux transducers are HFS-4 Heat Flux transducers (Omega Engineering). They were calibrated between two pieces of gypsum in a Laser Comp Fox 304 heat flow meter. For each HF transducer, seven different temperature gradients were established across the heat flow meter. Once the systems reached equilibrium, the heat flow was measured by the meter, and the voltage was measured with a USB-TEMP 24-bit data acquisition unit (Measurement Computing). A linear relationship was determined, and a heat flux coefficient was generated.

The data acquisition units employed were Measurement Computing USB-TEMP units with 24-bit resolution. The RH was measured with RH-USB (Omega Engineering). Weather recorded by a HOBO U30 (Onset) included wind speed and direction, rain fall, temperature, humidity, global radiation.

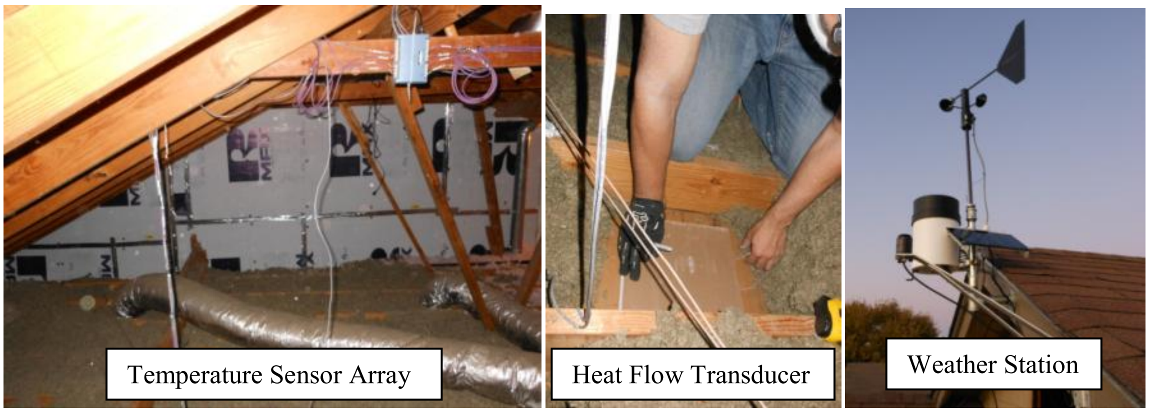

Figure 12. DAQ Components.

2.2 Radiation Control Technology Installations

As stated earlier, two types of low-cost radiation control strategies for southern U.S. applications were installed in tested attics: a) RB composed of an RB combined with an enclosed reflective air space, and b) spray-applied IRCC. Attic configurations are shown in Figure 10, where the IRCCs and RB were installed in the attic over the living spaces

2.2.1 Radiant barrier with enclosed airspace

Fi-Foil's Silver Shield is an insulating product composed of multiple layers of low-e materials designed to reduce radiant heat transfer. The inside layer is a metalized polymer with emissivity of 0.04 and the outside layer is reinforced aluminum foil kraft paper with emissivity of 0.03 bonded with a fire-retardant adhesive. The layers expand when installed to form a reflective air space to provide enhanced thermal performance (see Figure 13) and protect the low-e surface from the performance reducing effects of dust accumulation. Since metalized and foil-based aluminum products have a near zero water vapor permeance, Silver Shield is perforated to allow water vapor transmission.

In addition to the reflective properties of the product in attic application, the enclosed air space provides an R-value that increases the thermal performance of the attic insulation system. This product application reduces direct roof-deck level thermal loads and indirect attic floor heat transfer. This improves the thermal performance of HVAC ducts, and improves comfort levels in both winter and summer conditions.

Fi-Foil was installed in Duplex 2A by two to three labors. Equipment included scissors or utility knife, stapler, and measuring tape. Installation began approximately 1 in. to 2 in. above the attic floor mass insulation. The product was stapled every 4 in. to 8 in.. A 3 in. to 6 in. opening was left at the ridge and sections of Silver Shield were cut out for roof vents. Each end of the product was enclosed by folding the ends over twice to form a ¾ in. reflective air space.

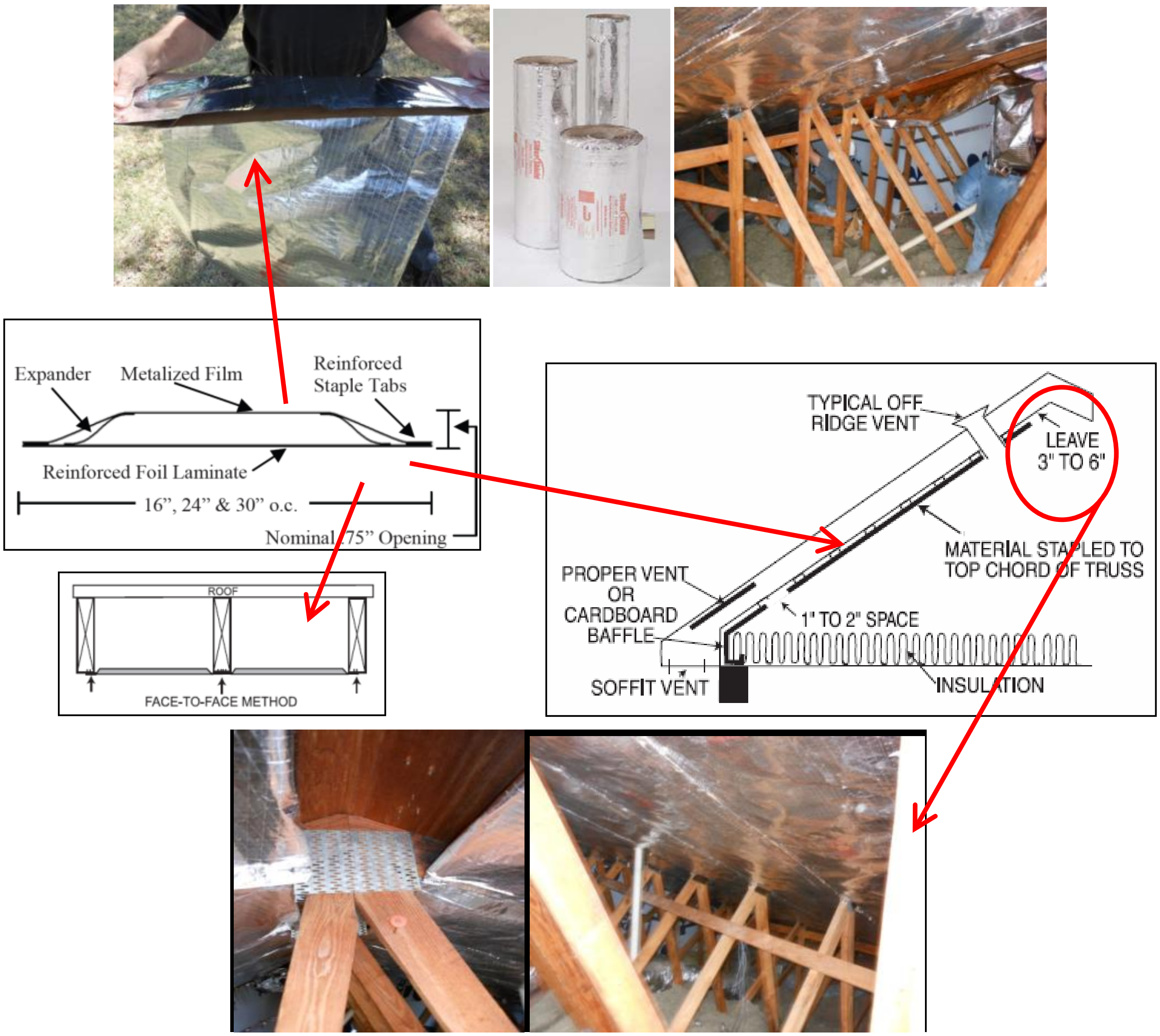

Figure 13. Installation of RB with enclosed airspace from Fi-Foil Company (Silver Shield).

2.2.2 Interior Radiation Control Coating (IRCC)

IRCC changes the emissivity of the surface where it is applied. Most building products such as plywood, brick, and plasterboard have high emissivities (0.70-0.95). When heated, they radiate most of their heat to cooler surfaces. LO/MIT IIMax can lower their surface emissivity, reducing their ability to radiate heat. Two IRCC products were applied in this project: LO/MIT-II MAX and HeatBloc-Ultra (see Figure 14).

I. LO/MIT-II MAX from Solec-Solar Energy Corporation

LO/MIT-II Max is a silver-colored, non-thickness dependent and low-e coating. When applied to building materials such as plywood, it lowers their surface emissivity to 0.17 or lower. LO/MIT-IIMax is water-based and is classified by ASTM as an Interior Radiation Control Coating System (IRCCS).

The coating was mixed thoroughly with a squirrel-cage mixer and pumped up through the gable end of Duplex 1. Alternatively, buckets could also be brought into the attic for application. The job was completed by one applicator in roughly three hours (including setup and cleanup time), covering the complete undersurface of the roof decking, including rafters, joists and gables/dividing walls. The worker used a filtered respirator and a Tyvek coverall suit for applicator protection. One coat was all that was required. Coverage was roughly 400 ft^2 of spray surface per gallon. After installation, the applicator can be cleaned up with water and soap.

No maintenance or re-coat is needed for the life of the roof deck. LO/MIT-IIMAX does not deteriorate or lose its optical properties over time and will not delaminate. It is permeable to moisture and is Class A Fire Rated for flame spread and smoke.

II. HeatBloc-Ultra from STS Coatings, Inc.

HeatBloc-Ultra is an aluminum-colored, water-based, low-e coating. When applied to building materials such as plywood, OSB or plasterboard, HeatBloc-Ultra lowers surface emissivity to 0.19 or lower. It is classified by ASTM as an IRCC.

In Duplex 2, the install time required approximately three hours from set-up to completion and clean-up. The crew consisted of two workers—one installer in the attic applying the material while another outside with the equipment and materials. Workers used safety precautions including a full-faced respirator, spray suit, hard hat and head lamp.

Figure 14. Installation of IRCC from Solec-Solar Energy Corporation (LO/MIT-II MAX) (left) and from STS Coating, Inc. (HeatBloc-Ultra) (right).

3 Experimental Data Analysis

As mentioned in the earlier sections, during the cooling season 2012, thermal performance measurements were performed on two residential duplexes (four housing units). Since the major goal of this project was to evaluate the energy effects of RBs and IRCCs, these field tests focused on thermal and energy performance of the attics. As a result, three test attics were modified using RBs and IRCCs and tested. The fourth attic stayed unmodified and was used as a baseline for comparisons. To reiterate, the primarily goal was to investigate performance of the attic thermal components, not an attempt of the complete whole building energy retrofit. Therefore, results presented herein should not be considered as whole building retrofit strategies. However, the findings of this project can be useful in the future for development of energy conservation strategies for whole buildings, including building retrofit projects.

A major goal of this part of analysis was the thermal performance comparisons of three radiation control technologies used in the field testing. This section shows thermal performance data collected during three different time periods of significantly different exterior temperatures and levels of insolation—April, June/July, and July/August 2012. Note that all test housing units were occupied during the testing by families. Each of these families had different occupation habits and thermal comfort preferences. In each house, thermostat temperature setups were close, but not identical. Also, individual schedules for using the AC were different. In addition, the duplexes—even though they had been similarly built in relatively close time periods—had attics with different structural components, thicknesses, types of attic floor insulation and levels of attic ventilation.

In the following sections, the recorded test data is presented and compared for all four test units. Significant attention was paid to the comparison of the attic air temperatures, which were considered (due to the listed above differences in the attic construction) as a best indicator of the performance differences between analyzed technologies.

The following data is summarized and analyzed below:

- External and Internal Air Temperature Comparisons
- Experimental Attic Temperature Comparison
- Experimental Heat Flux Comparison
- Theoretical Heat Flux Comparison.

3.1 External and Internal Air Temperature Comparisons

As mentioned earlier, thermal performance comparisons were conducted for three major time periods: 1) April - when exterior air temperature was below 30°C for most of the day, reaching 10°C during the nights; 2) June/July – with the highest daily temperature peaks, and 3) July/August, with typical summer temperatures and insolation levels. The overnight temperatures during the mid-summer months were relatively close with minimal oscillating between 12°C and 15°C.

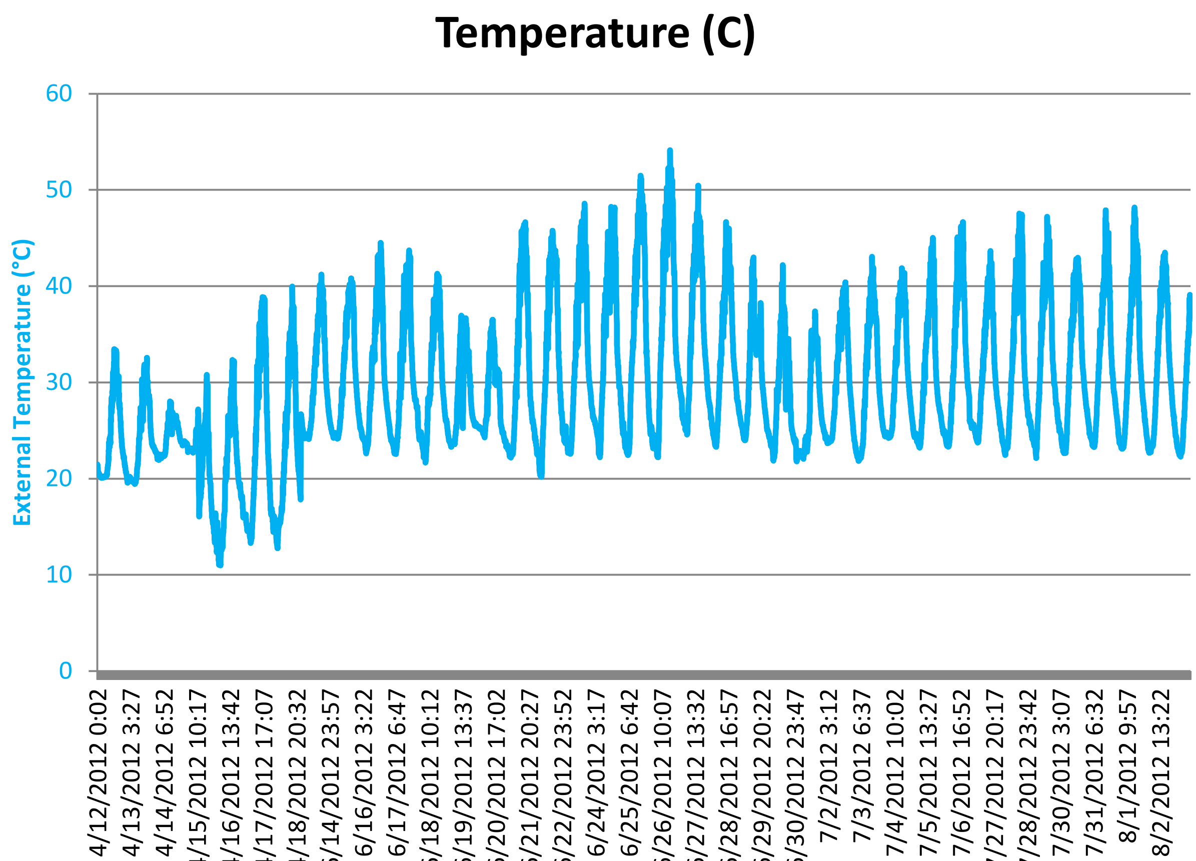

Figure 15. Measured exterior air temperature on one of the test houses.

As shown in Figure 15, the weather data displays the external temperature varying between 10°C during the night, and approximately 52°C during the day. It was also observed that during the mid-summer months, minimum night temperatures stayed above 20°C.

As mentioned in previous sections, the orientations of test houses were very close and all test attics had similar roof finish materials using plywood decks and asphalt shingles. These facts helped in thermal performance comparisons for the top parts of the roof assemblies. Figures 16-21 show basic comparisons of the top of the roof temperatures in all four test units. These temperatures represented the top-level boundary conditions for the roof/attic structures. They were critical for calculation of the thermal loads generated by the roof and estimation of the overall performance of the attic thermal system (insulation, attic ventilation rates, and radiation control technologies).

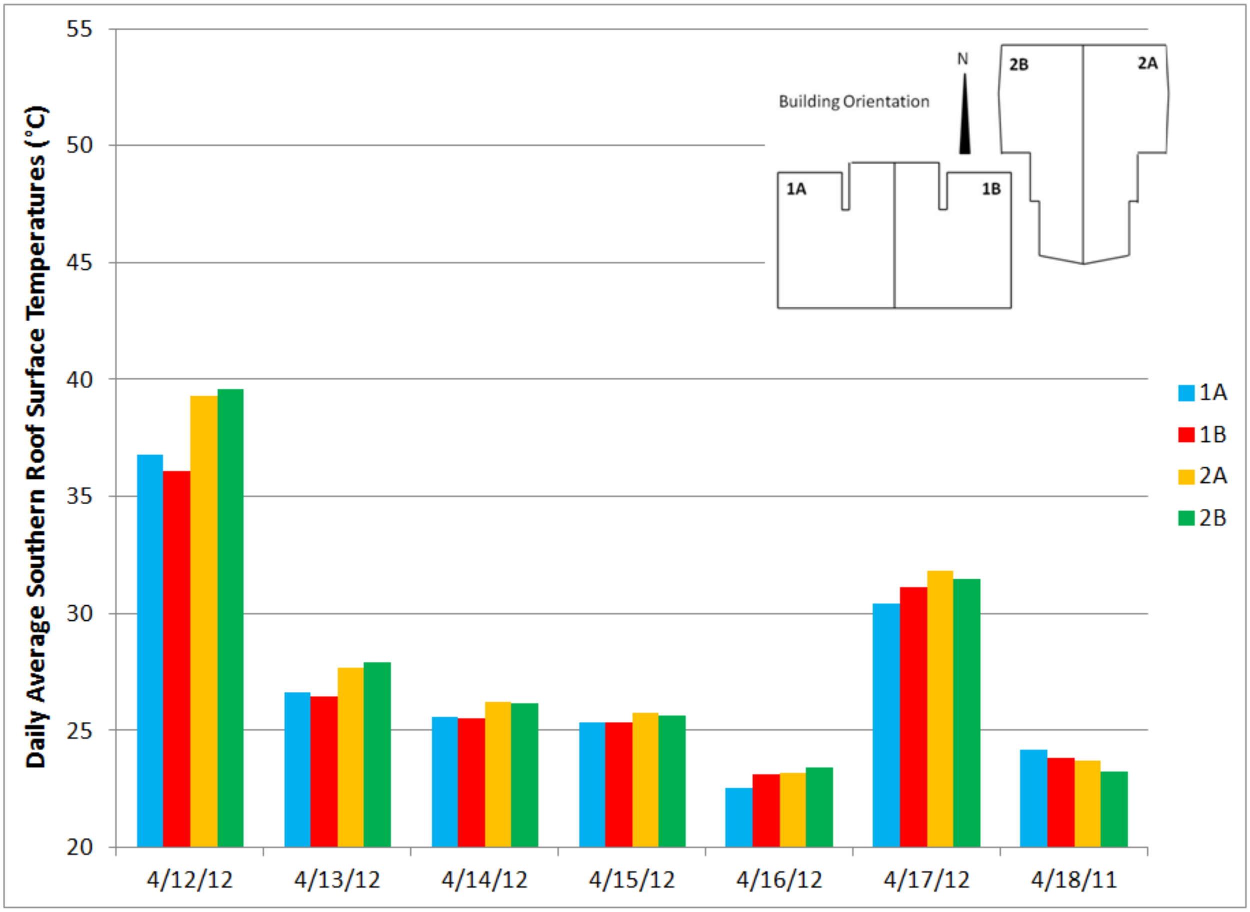

Figure 16. Average daily roof surface temperatures recorded during the April measure period.

Figure 16 displays the averages of the roof surface temperatures recorded in April 2012. Although they varied greatly by day, up to 20°C for the period, the temperature trends were not large or consistent. At times, the roof of Duplex 2 was on average 1°C-2°C warmer than that of Duplex 1.

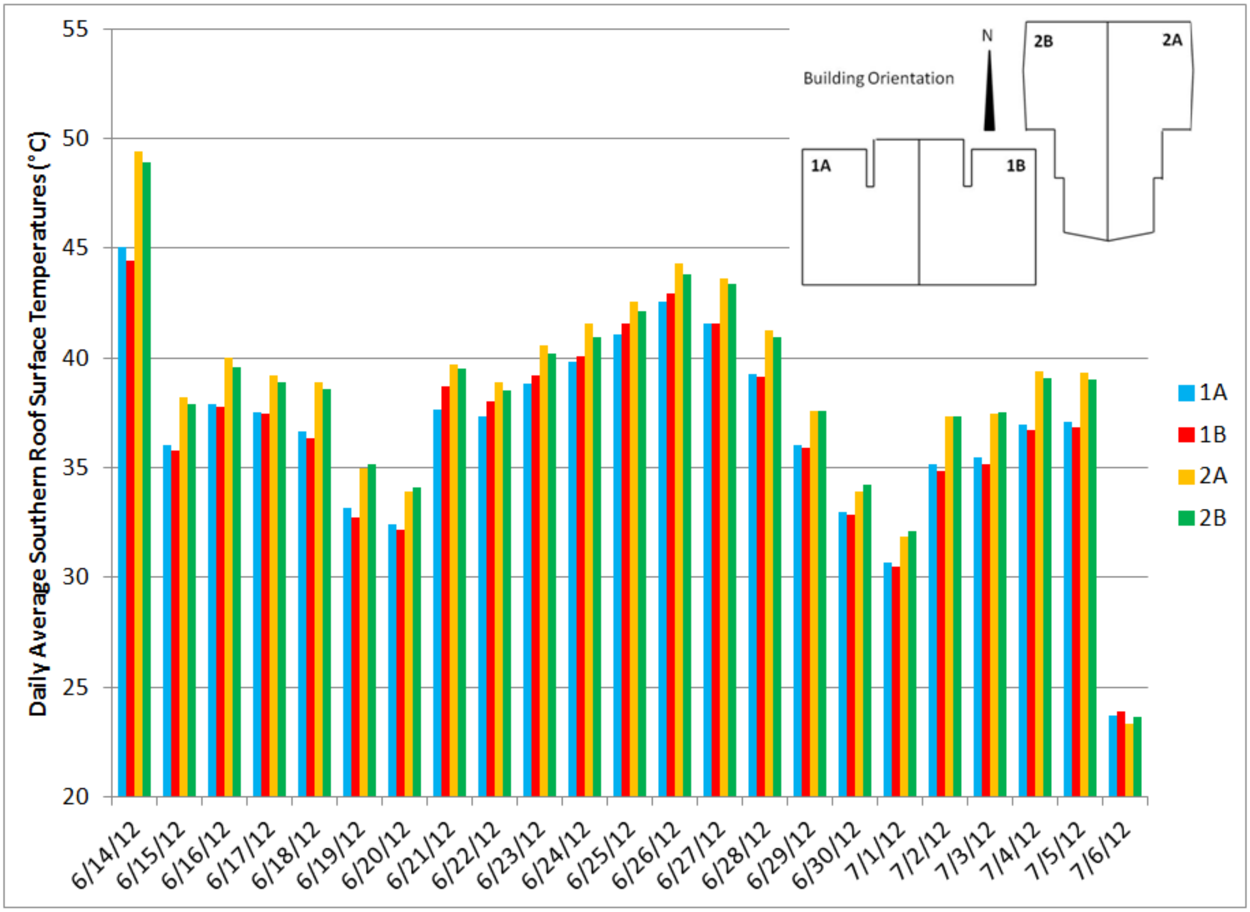

Figure 17. Average daily roof surface temperatures recorded during the June/July measure period.

For most of the June month, the average temperatures recorded on the roof surfaces were between 15°C and 20°C higher than temperatures recorded during the April period. As seen in Figure 17, in June the roof temperatures of Duplex 2 were typically 1°C to 2°C warmer than Duplex 1. This small difference was most likely caused by notable differences in attic ventilation systems used in both duplexes. The other reason might have been the different structural components in both duplexes, which interfered in a different way with radiation heat exchange between the roof deck surface and the top of the attic floor insulation. In addition, Unit 2A typically had the highest roof temperature. This roof used an aluminum foil RB with two enclosed air gaps just under the roof deck surface (one enclosed space between two RB layers, and one enclosed layer between RB and underside of the roof deck). For this reason, the temperature balance in this area was different, compared to other test attics. The greater roof surface temperature might have been a consequence of this fact.

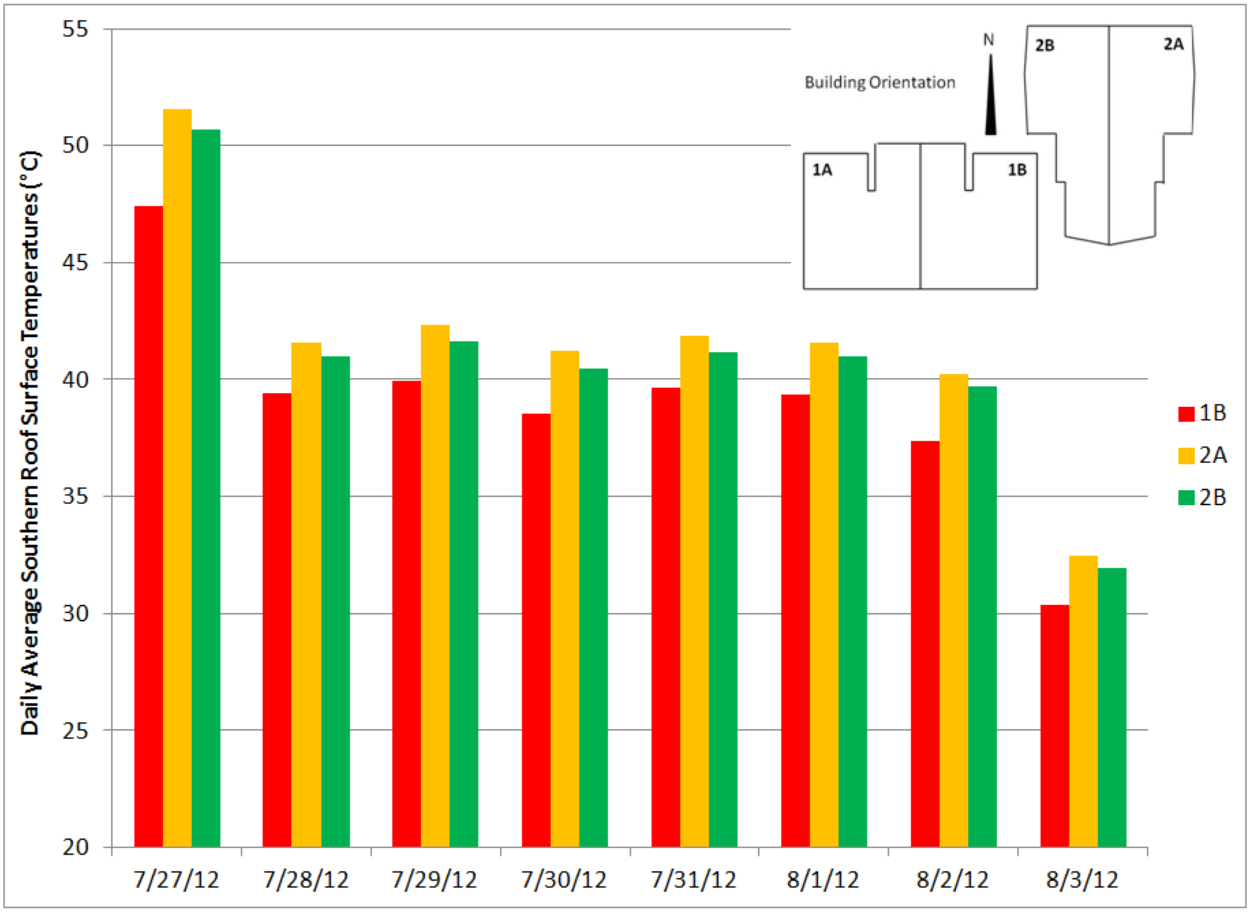

Figure 18. Average daily roof surface temperatures recorded during the July/August measure period.

The temperatures of Duplex 2 were consistently higher than Duplex 1, as seen in Figure 18. This was the most pronounced during the hotter months of June and July. In general, however, the roof surface temperatures were very similar with differences seldom reaching 3°C.

In summary, data presented in Figures 16, 17, and 18 indicate notable differences in thermal performance of the top of the roof in all four test units. These differences were caused by dissimilar ventilation rates followed by varying structural and insulation components in Duplexes 1 and 2. However, yielded temperature differences between these individual units did not exceed 2°C for most of the time during the summer 2012. The highest temperature of Duplex 2A's roof was caused by the aluminum foil RB containing two enclosed air gaps (one enclosed space between two RB layers, and one enclosed layer between RB and underside of the roof deck). This thermal system was installed just under the roof deck surface reducing the amount of heat transmitted from the roof surface down to the attic space.

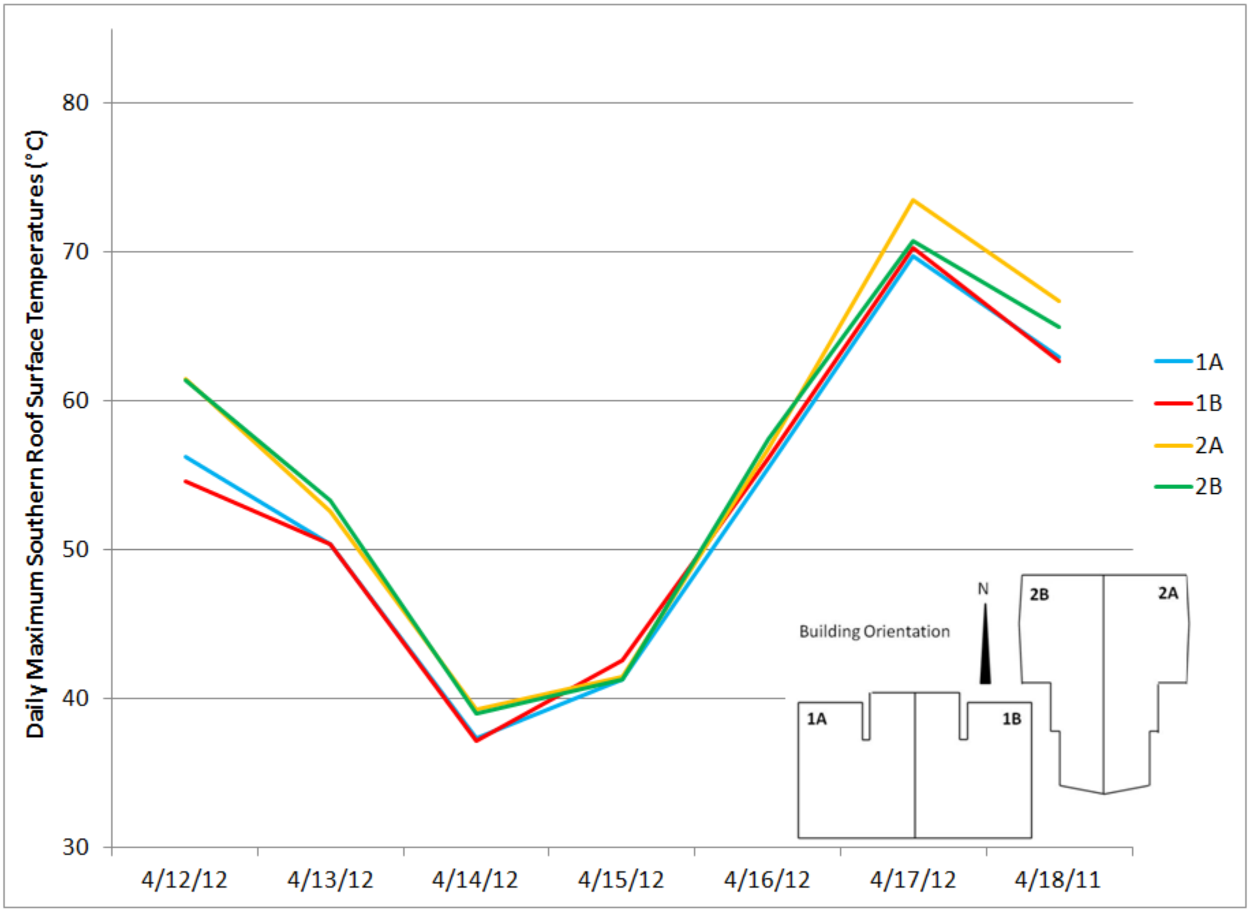

Figure 19. Maximum roof surface temperatures recorded during the April measure period.

Roof-generated daily peak-hour thermal loads were a function of the maximum roof temperatures. The higher the roof surface temperature, the higher thermal load was transmitted to the attic space. As seen in Figure 19, the maximum roof surface temperatures for all four test units in April were very similar and varied greatly between 40°C and 70°C. Similarly, as in earlier figures, the temperatures of Duplex 2 were typically higher than in Duplex 1.

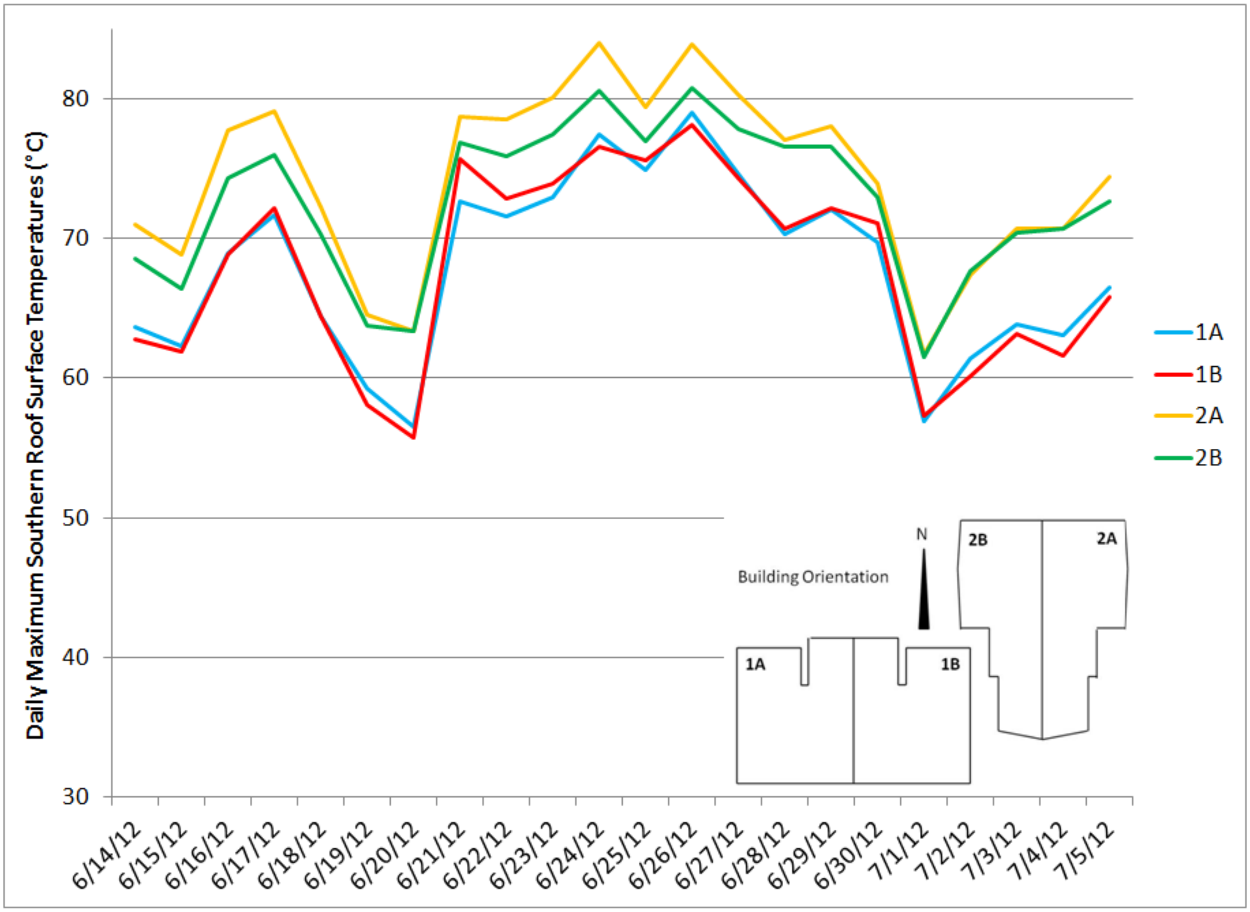

Figure 20. Maximum roof surface temperatures recorded during the June/July measure period.

Again, when the weather becomes warmer in June, the roof temperatures of Duplex 2 were greater than Duplex 1. The maximum roof temperatures in June for Duplex 2 were up to 5°C hotter than Duplex 1. This was most likely due to general differences in construction of both types of attics and thermal behavior of the RB combined with the enclosed air gaps, installed under the roof deck in the test house 2A.

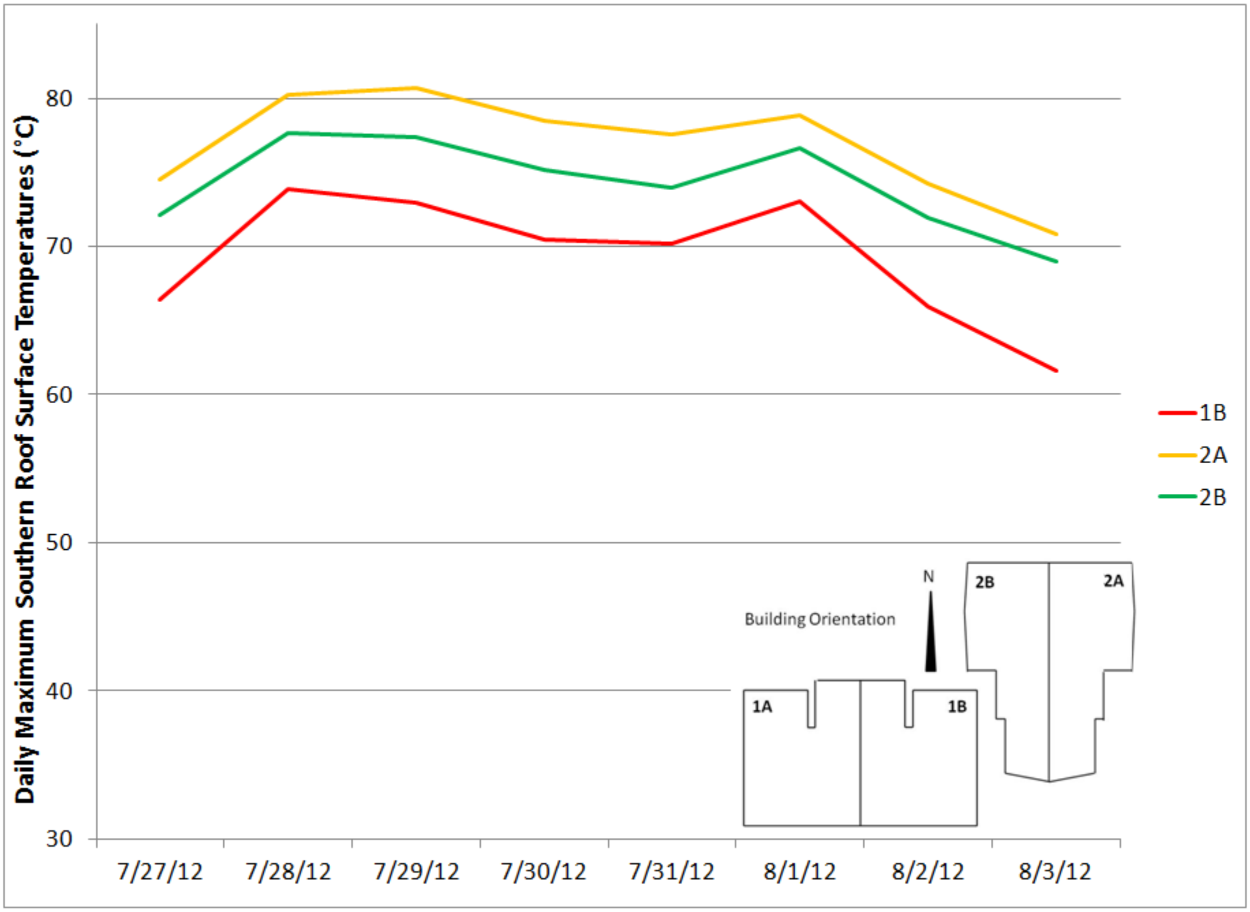

Figure 21. Maximum roof surface temperatures recorded during the July/August measure period.

It is clear from Figure 21 that the differences between the houses became more pronounced when looking at the maximum roof surface temperatures. The maximum roof surface temperatures in July varied by 3°C-4°C across Units 1B, 2A, and 2B. This was similar to previous charts where the foil technology in 2A had the hottest roof temperature and the IRCC in 2B had slightly higher roof temperature than in Unit 1B.

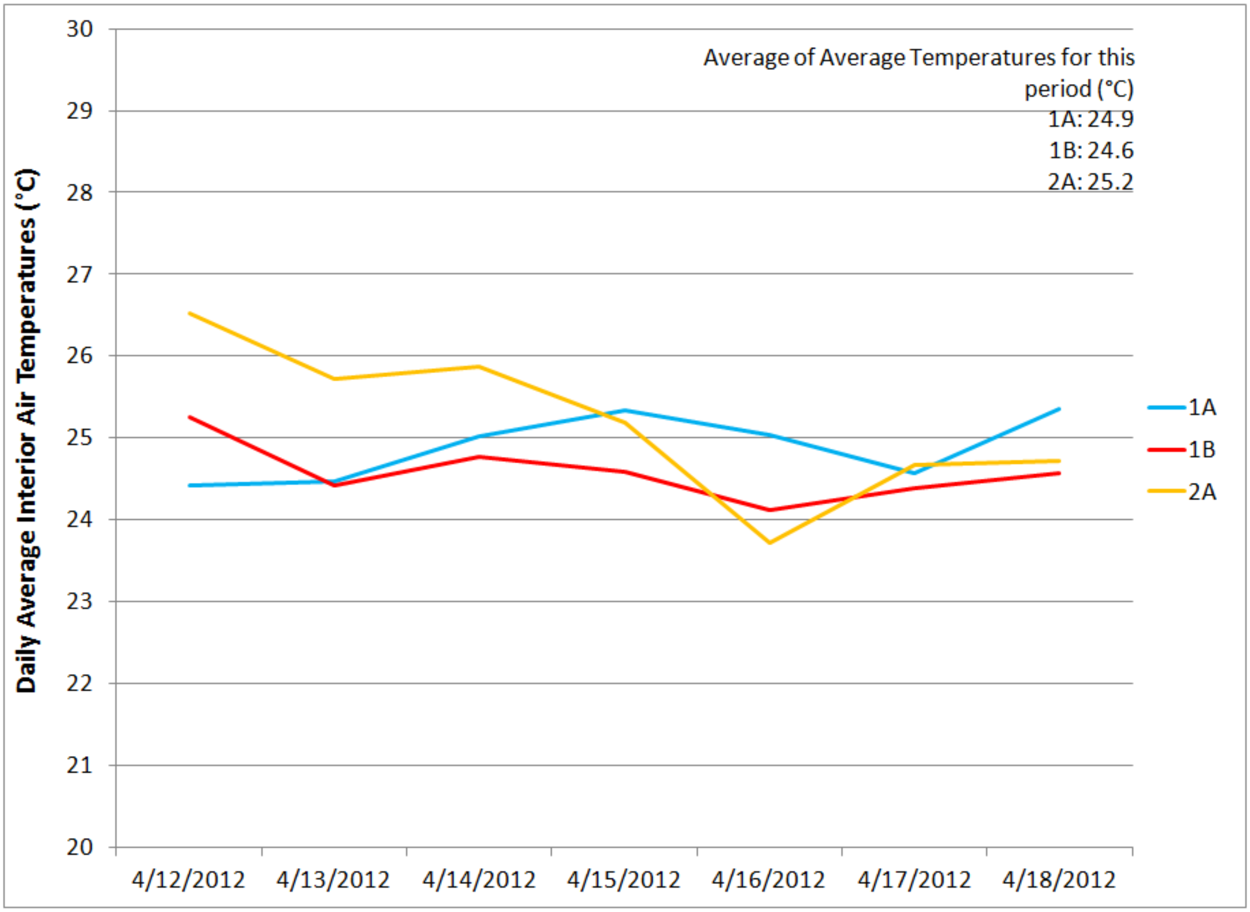

Figure 22. Average interior air temperatures recorded during the April measure period.

As mentioned earlier, all test units were occupied during the testing. Each of these families had different occupation habits and thermal comfort preferences. In each of these houses, thermostat setups were close but not identical. As shown in Figure 22, the beginning of the cooling season for residents of Unit 2A was most likely on April 15. Also, individual schedules for using AC were different for each test unit. In April, the internal air temperatures were close to 25°C, as seen in Figure 22.

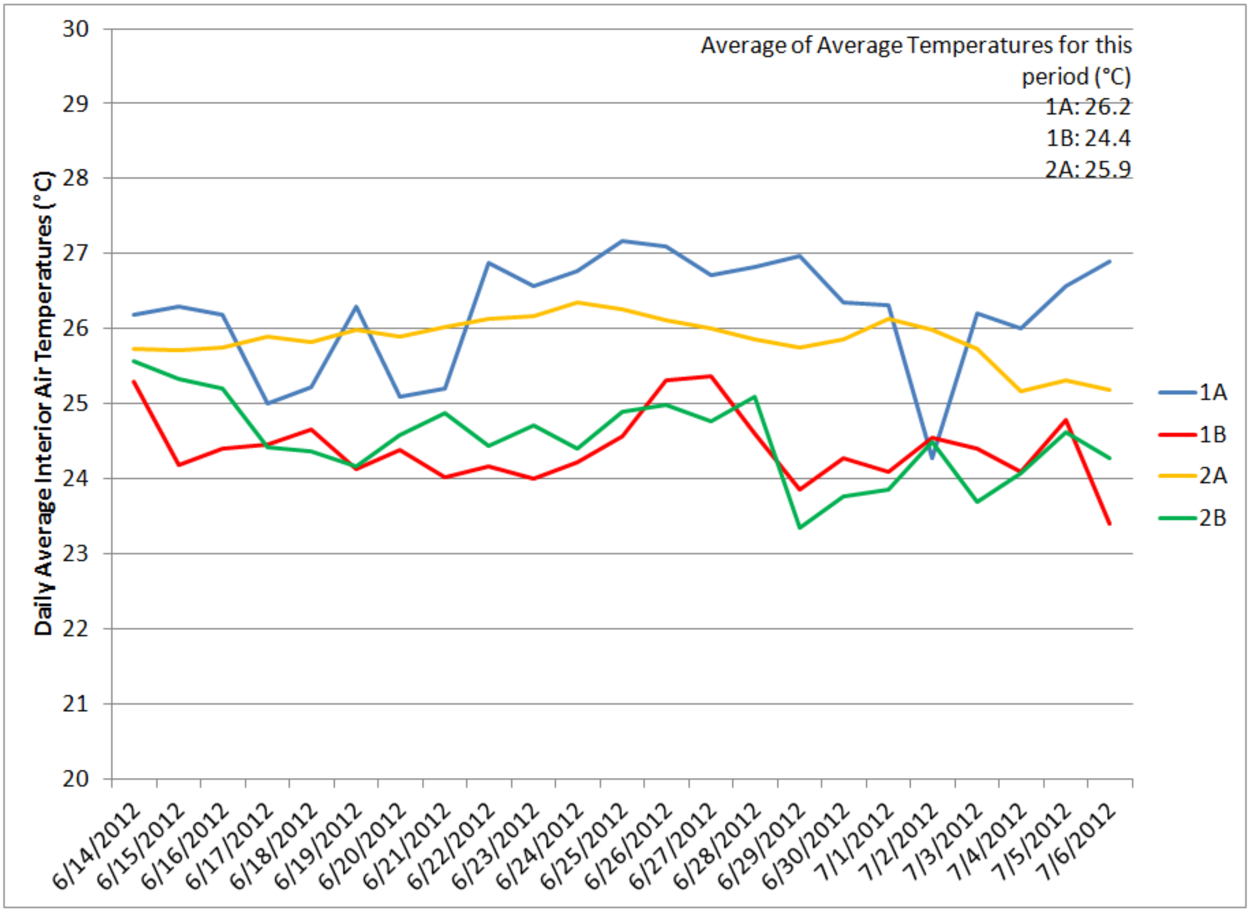

Figure 23. Average interior air temperatures recorded during the June/July measure period.

Figure 23 displays that the internal temperatures were close to 25°C in June, as well. Most likely, residents of Units 1A and 2A preferred interior temperatures slightly above 25°C, while residents from Units 1B and 2B preferred temperatures closer to 24°C.

3.2 Experimental Attic Air Temperature Comparisons

Typically in residential attic applications, RBs and IRCCs work by reducing the amount of thermal radiation that is transferred across the air space between the roof deck and the top of the attic floor insulation. Since the amount of thermal radiation increases as the temperature of the emitting surface increases, it is critical to keep it as low as possible. This surface can be directly roof deck, foil-laminated roof deck boards, roof deck boards coated with IRCC, or RB material facing the interior of the attic. An application of multifoil RB in the case of Unit 2A showed that sometimes it was possible to apply radiation control technology, increase the roof deck temperature and at the same time reduce the air temperature in the attic. As depicted in Figures 17–21, this technology generated a slightly higher roof surface temperature compared to other test attics. However, when attic air temperatures were compared, the recorded attic temperature for Unit 2A was significantly lower comparing to other attics; see Figures 25, 26, 27, 28, and 29 below.

In this project, due to the structural differences between the test attics and due to the fact that the attic floor insulations were not uniform in all the units, measurements of the attic air temperatures in the center-of-the-attic location were used as one of indirect indicators of the attic system thermal performance. The second potential performance indicator considered in this project was heat flux measured on the ceiling level. However, as shown in Figures 22 and 23, the internal air temperatures were not identical in all test units. That is why direct comparisons of measured heat fluxes cannot be used as a full indicator of the attic system thermal performance.

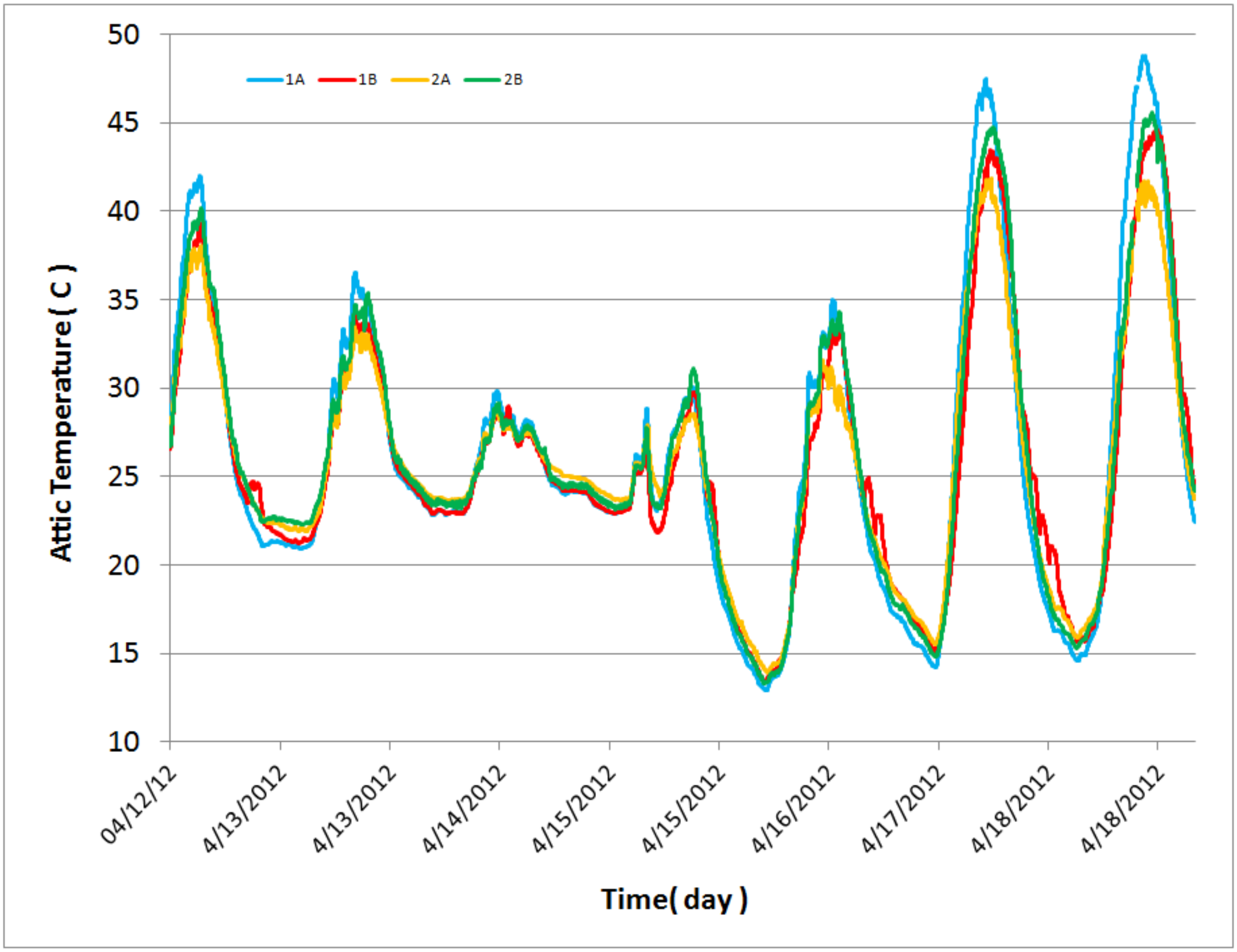

Figure 24. Example of attic air temperatures recorded in four test attics (center location) during the April measure period.

The charts in Figure 24 display the general appearance of attic temperature data collected for Duplexes 1 and 2. The temperatures varied between 13°C during the night and 47°C during the daytime. About a one-hour time delay was observed between maximum temperature peaks recorded in 2A's attic (with multifoil system) and other attics.

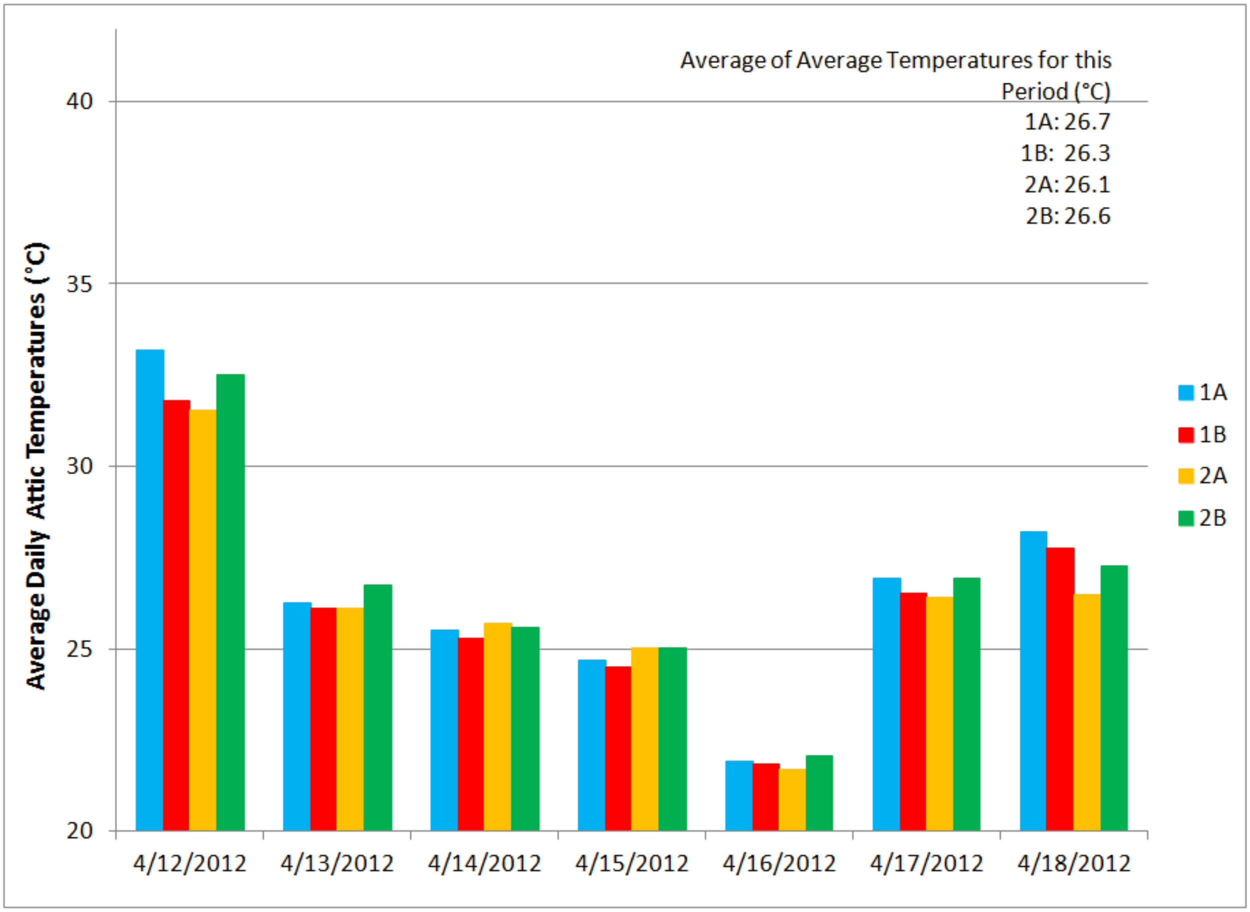

Figure 25. Average daily attic air temperatures recorded in four test attics (center location) during the April measure period.

The differences in attic temperature in April were small and not consistent, as seen in Figure 25. Attic air temperature oscillated between about 33°C and 22°C during the April measure period. During the warmest days, attic 2A, containing multifoil RB, was the coolest attic among all tested units.

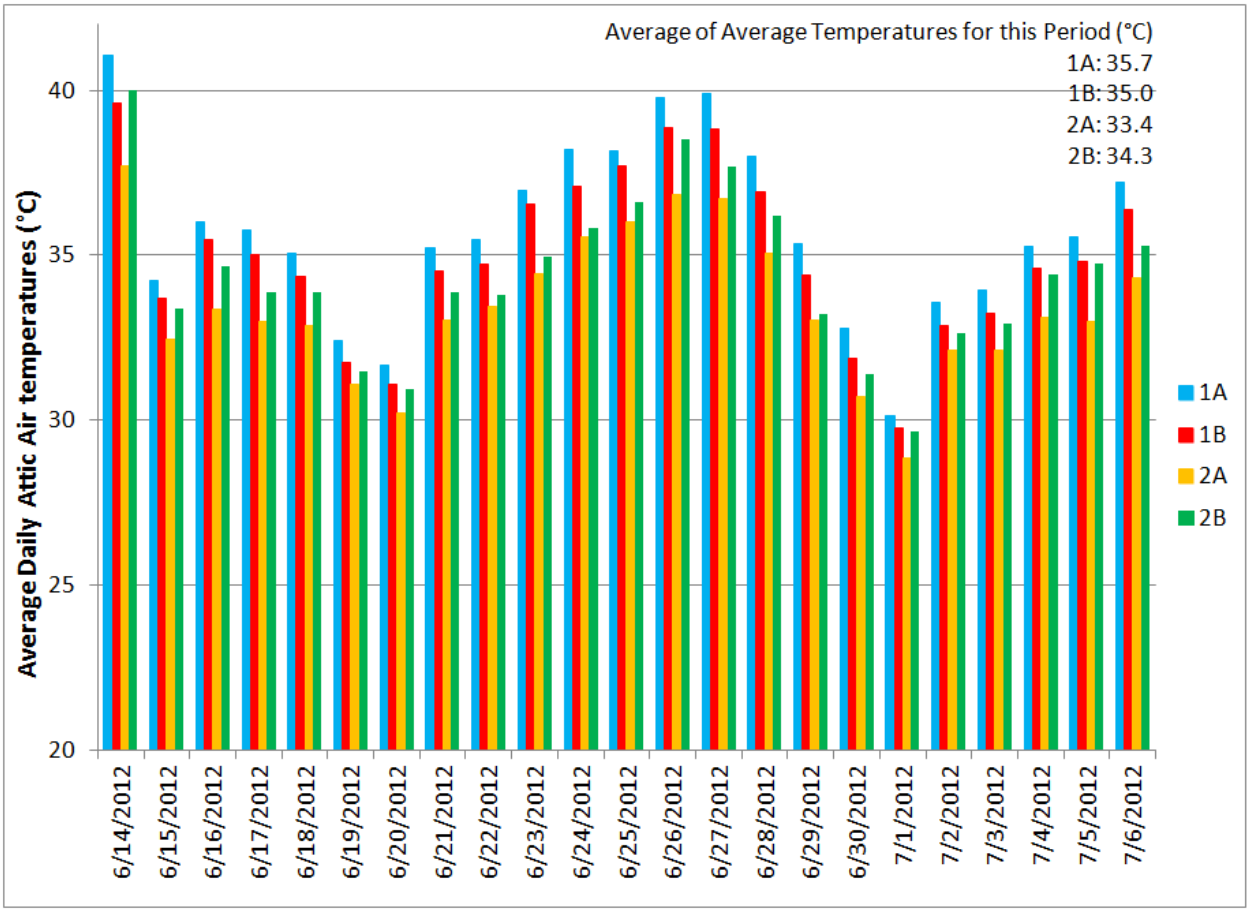

Figure 26. Average daily attic air temperatures recorded in four test attics (center location) during the June/July measure period.

Figure 26 shows that the attic of Duplex 1 was typically hotter than Duplex 2 in June 2012. This is consistent with the observation that the roof of Duplex 1 was cooler than Duplex 2. It is good to remember that there were some differences between both duplexes, such as the roof deck construction—rafters versus trusses—and the levels of ventilation in the attics, determined by measuring the area of the soffit vents. An average baseline attic temperature for the considered time period was 35.7°C, while for the coolest attic 2A was only 33.4°C. This was a 2.3°C difference.

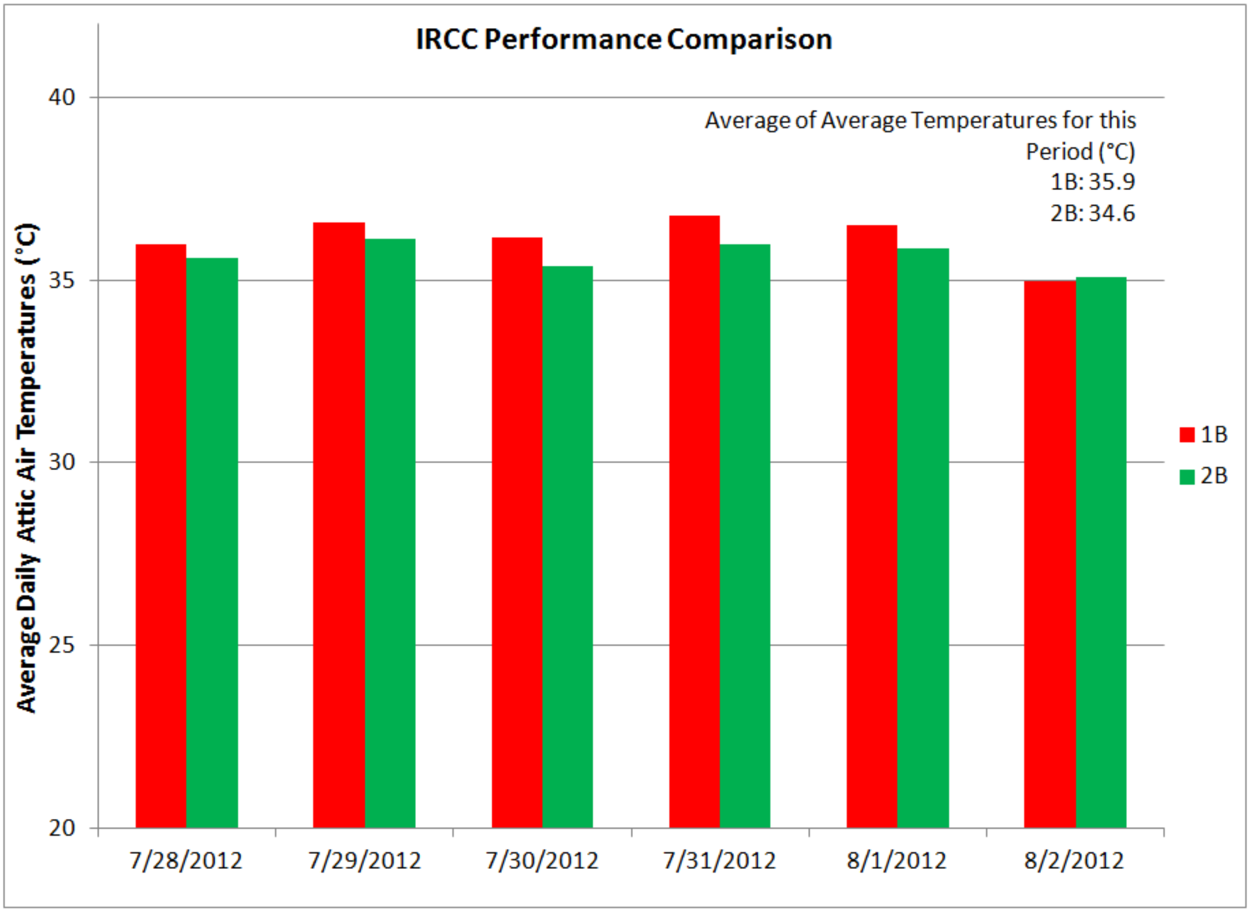

Figure 27. Average daily attic air temperatures recorded in two IRCC attics (center location) during the July/August measure period.

For the hottest month of the year, Figure 27 shows that the average attic temperature was very similar between the two IRCC technologies. The temperature in 2B was slightly lower than 1B, by approximately 1°C. This might be caused by construction differences between Duplexes 1 and 2.

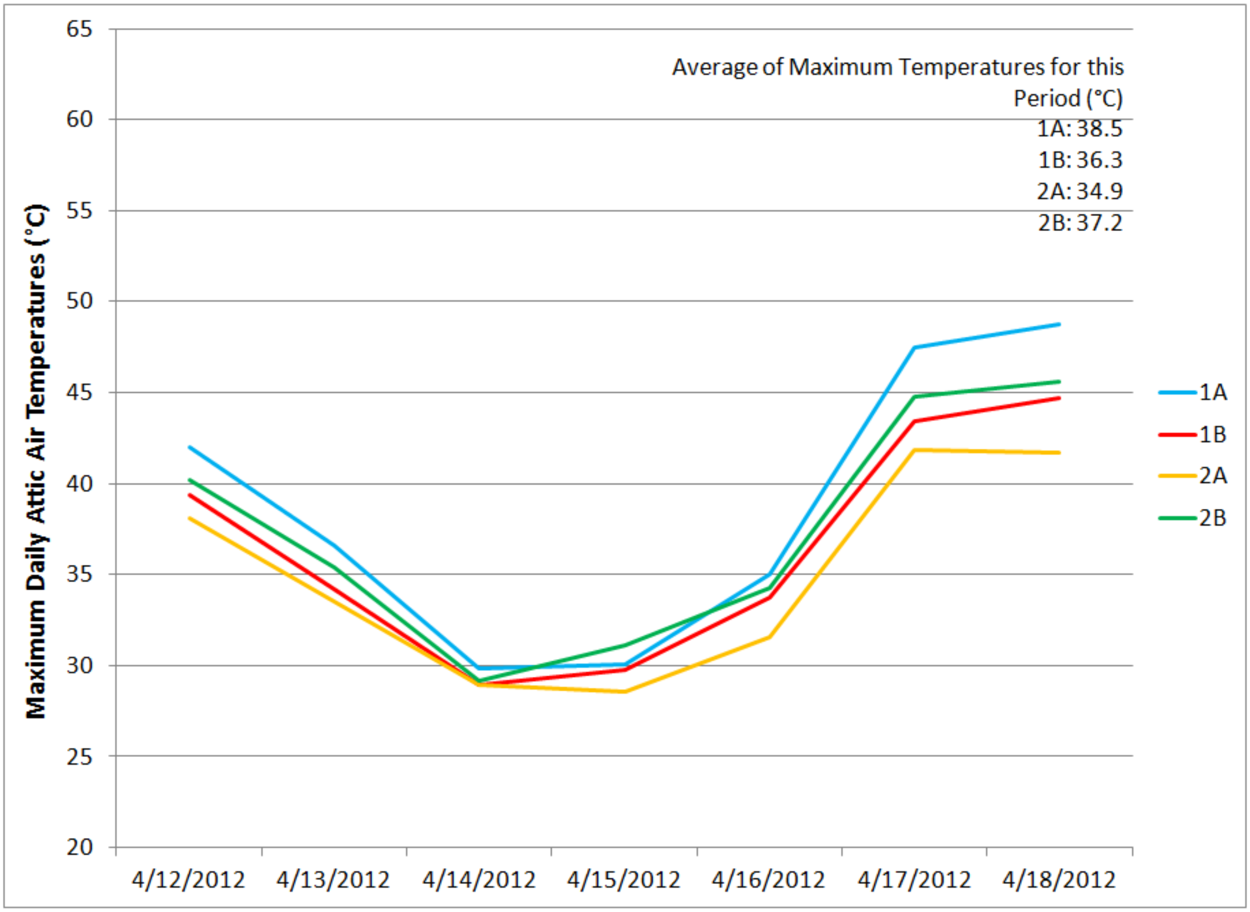

Figure 28. Maximum daily attic air temperatures recorded in four test attics (center location) during the April measure period.

The maximum attic air temperatures were similar in April, generally varying by a degree or less, as seen in Figure 28. During the last, warmest day of the period the temperature difference between the hottest (1A) and coolest attic (2A) was close to 8°C. Average attic air temepratures were within 3.6°C.

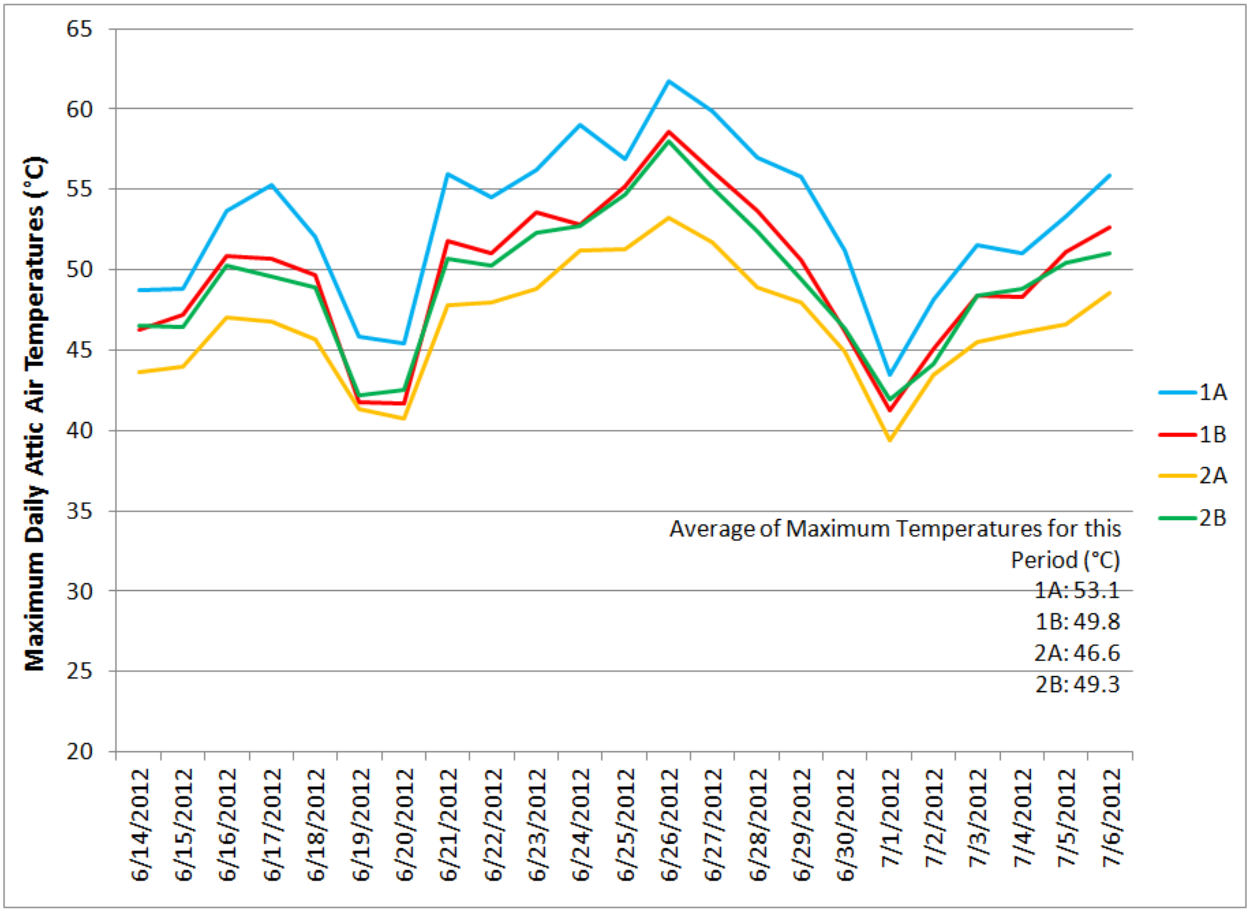

Figure 29. Maximum daily attic air temperatures recorded in four test attics (center location) during the June/July measure period.

Figure 29 depicts the maximum daily attic air temperatures for June/July 2012. These temperatures reflect differences in attic-generated peak-hour cooling loads during the day. It is clear that different types of reflective insulation work effectively in southern U.S. climates. In June, the base case attic, 1A, had consistently higher maximum daily attic air temperatures. Units 1B and 2B were quite similar, but were generally a lower maximum temperature than the base case (over 3°C on avarage). The fact that 1B and 2B appeared similar was a different pattern than previously observed. However, examining the hotter time period in July may confirm that 2B generally had lower attic temperatures than 1B. Finally, 2A,the house with the foil technology installed, had the lowest maximum temperatures across this period by approximately 7°C, while compared to the baseline attic, 1A.

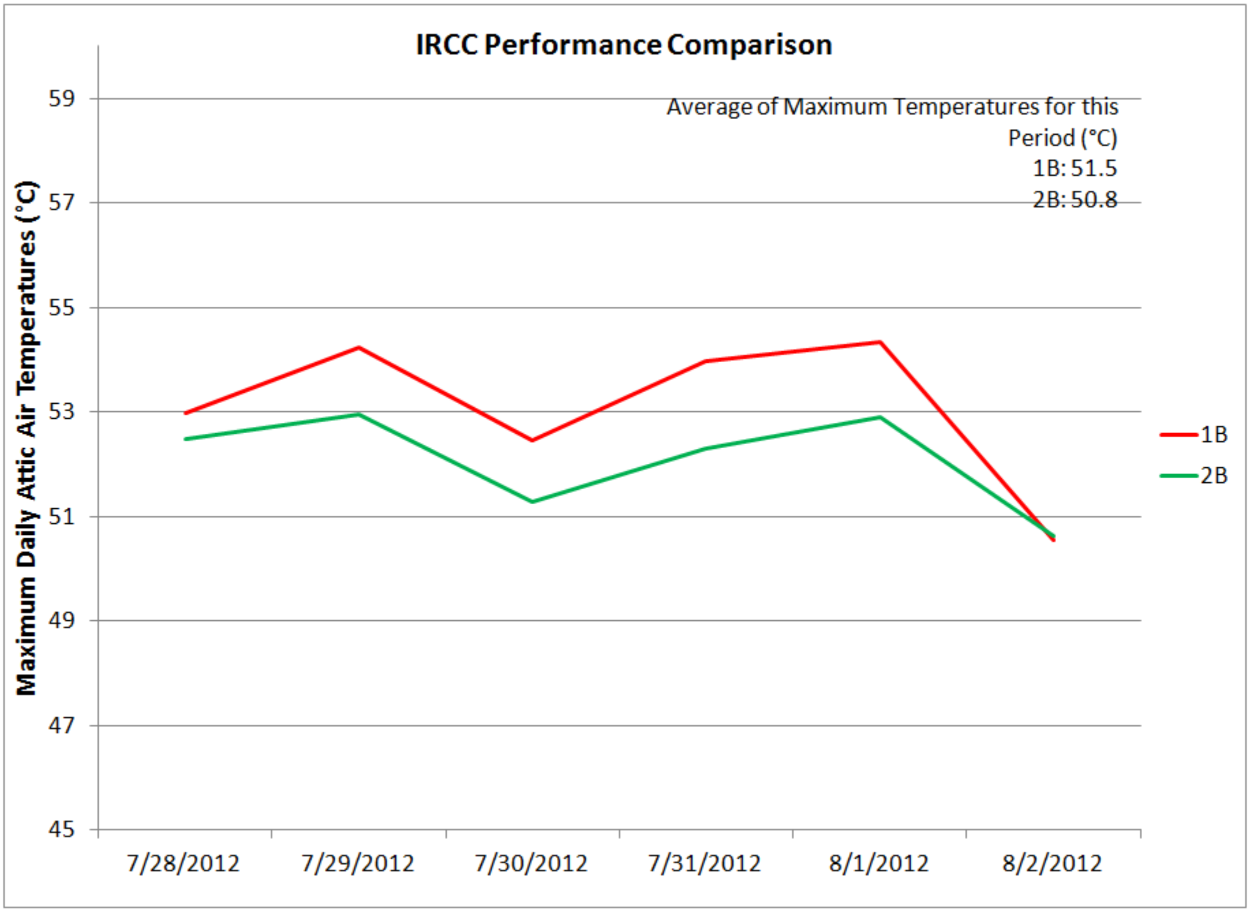

Figure 30. Maximum daily attic air temperatures recorded in two IRCC attics (center location) during the July/August measure period.

As shown in Figure 30, the attic with the IRCC technology installed in the Duplex 2 had lower maximum temperatures across this time period, while comparing to the similar attic in Duplex 1. Even for hottest summer days, 2B and 1B had very similar maximum attic temperatures with differences not exceeding 1°C.

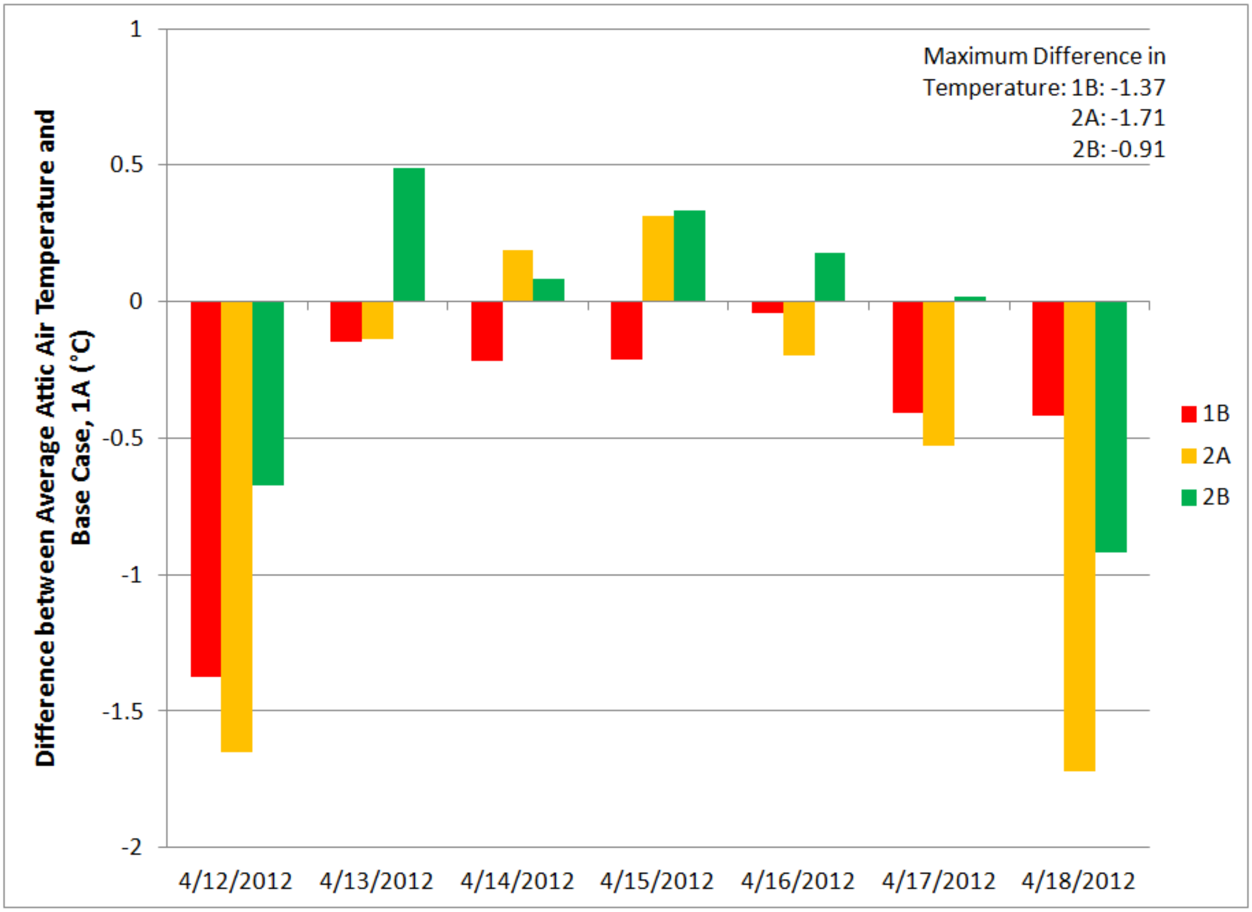

Figure 31. Differences in daily attic air temperatures recorded between three test attics using radiation control technologies and a baseline attic, during the April measure period.

As mentioned earlier, field measurements of the attic air temperatures were used in this project, as one of the indirect indicators of the attic system thermal performance. It can be said that the attic air temperature represented thermal condition equilibrium incorporating radiation, ventilation, and convection effects together. This temperature also reflected structural differences between all test attics.

Figure 31 displays the difference between the average attic air temperatures for the houses with technology—Units 1B, 2A and 2B—and the base case attic. The most extreme values indicate the greatest differences from the base case. The only consistent observation in this chart is that the attic in Unit 2A had the most different attic temperature from the base case.

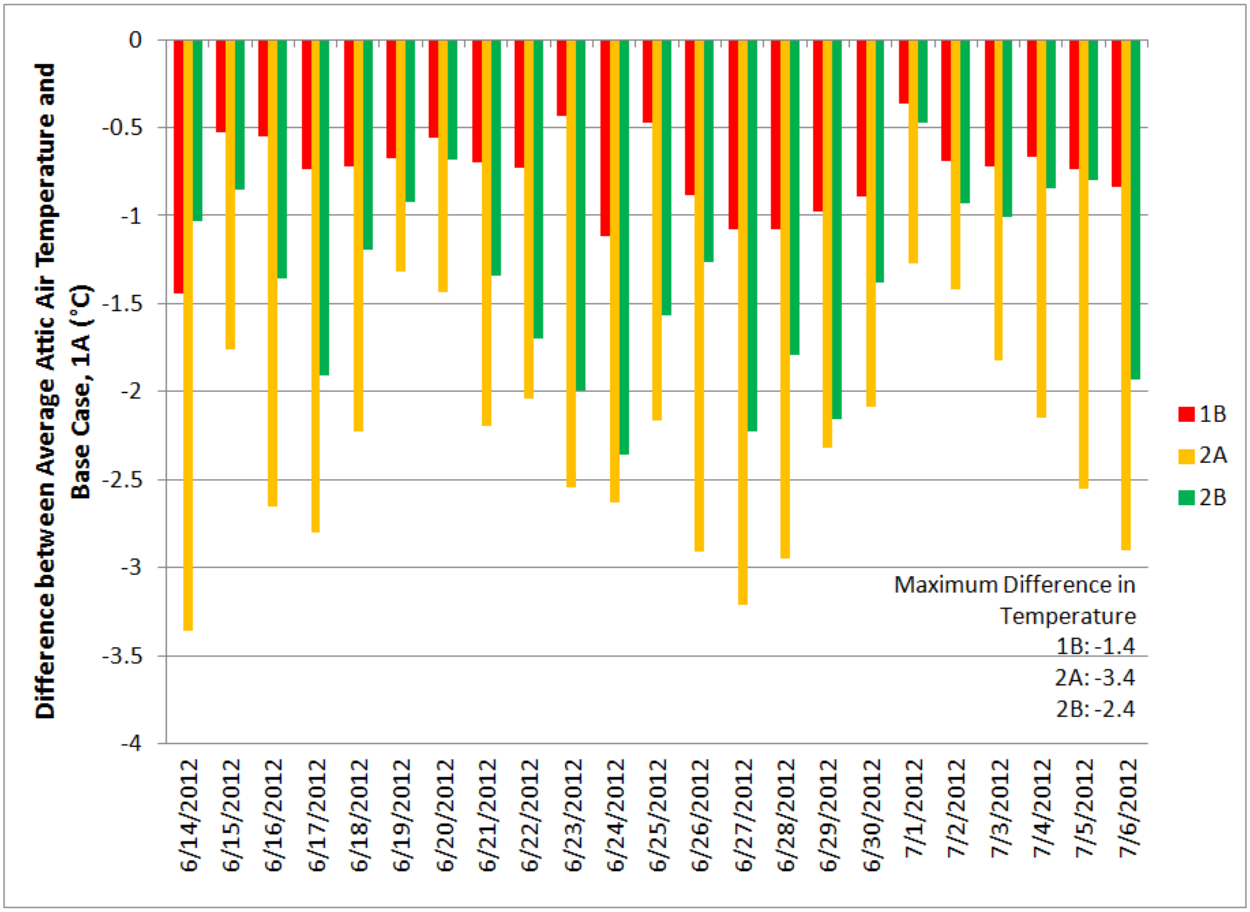

Figure 32. Differences in daily attic air temperatures recorded between three test attics using radiation control technologies and a baseline attic, during the June/July measure period.

The chart in Figure 32 indicates that the foil technology was thermally more effective than both IRCC technologies. An average temperature difference between this attic and the base case was about 3.4°C, while for the IRCC technologies, it was about 2°C. In addition, the IRCC in 2B was usually more different from the base case than the 1B case.

It is important to note that 3.4°C reduction of the average attic air temperature caused by the multifoil RB can be an equivalent to more than 34% reduction of the attic-generated cooling loads—assuming approximate steady-state heat transfer, average attic temperature of 35°C (as shown in Figure 26) and internal air temperature of 25°C. It has been reported that for U.S. residential houses, roofs and attics generate an average of 12% cooling energy contributions (Huang et al., 1996). In that light, potential whole building cooling energy savings may reach about 4%, depending on other building parameters and HVAC system efficiency.

Similarly, a 2.4°C reduction of the average attic air temperature due to the IRCC technology can be an equivalent to more than 24% reduction of the attic-generated cooling loads. Potential whole building cooling energy savings for this technology may be close to 3%.

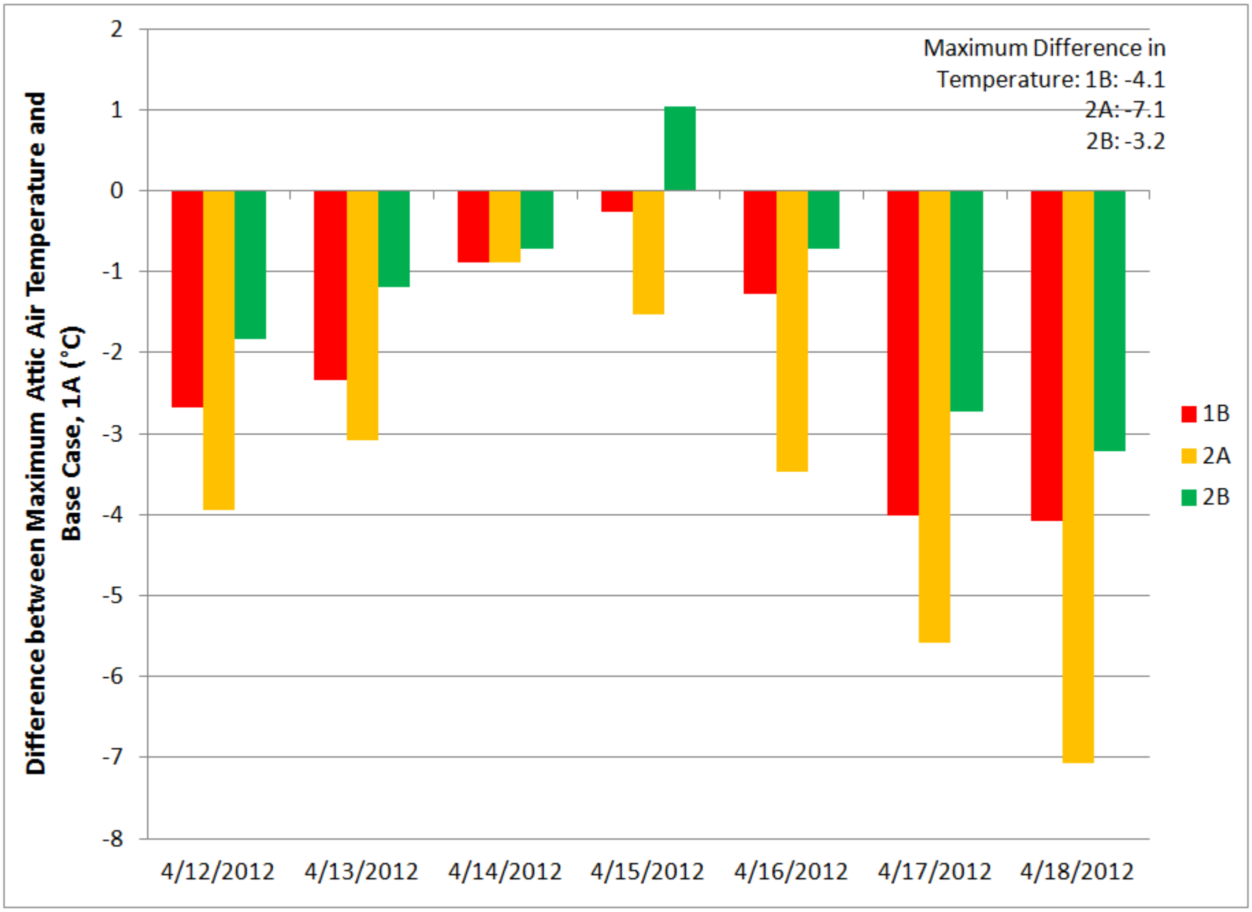

Figure 33. Differences in maximum daily attic air temperatures recorded between three test attics using radiation control technologies and a baseline attic, during the April measure period.

Figure 33 displays the difference from the base case for the maximum attic temperatures. Unit 2A, being the most extreme, had temperatures that varied the most from the base case. The maximum air temperatures for the attic using the multifoil system were on average about 7°C lower from the base case attic.

Surprisingly, the IRCC attic, 1B, showed more difference from the base case than 2B. This was different from previous observations, where 2B generally had lower temperatures than 1B and the base case had very high attic temperatures.

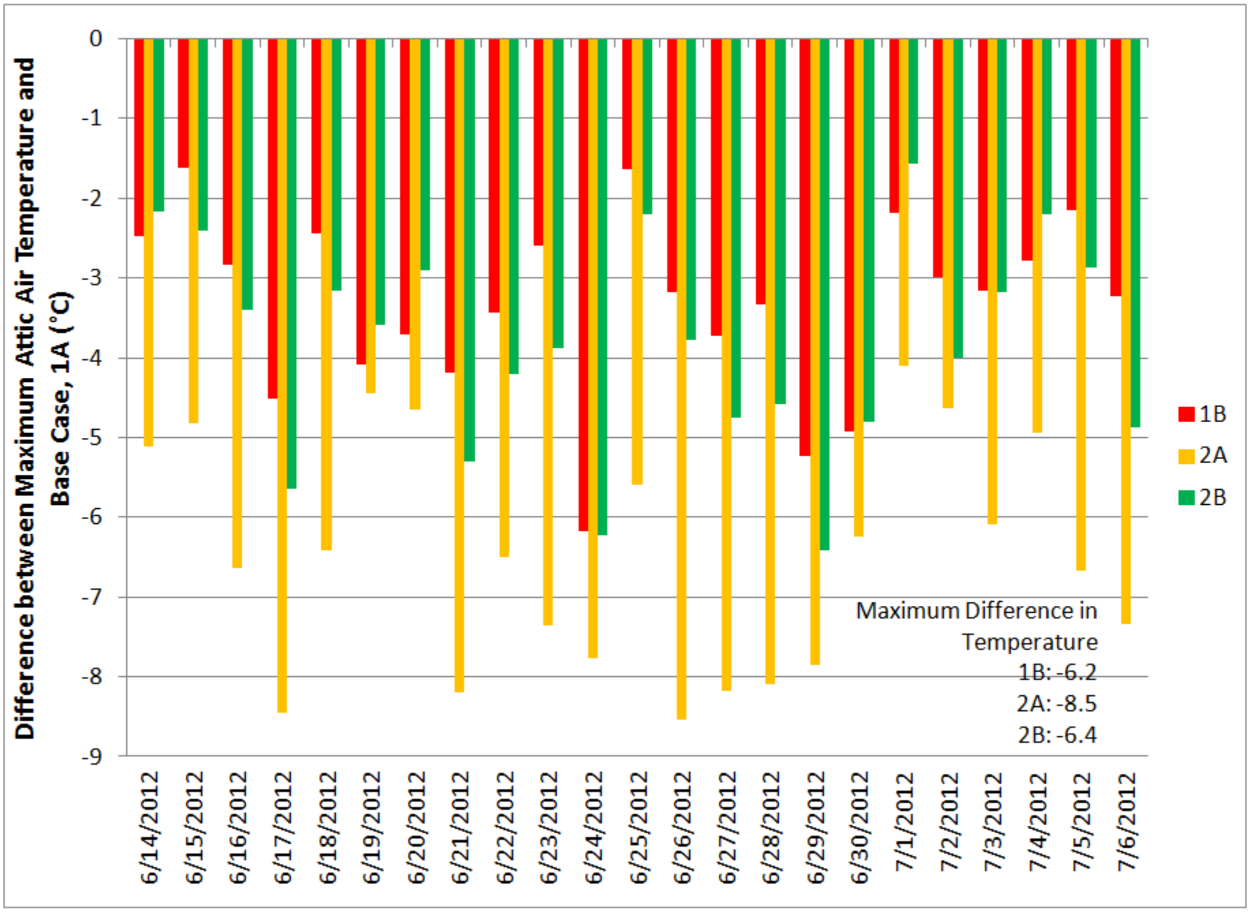

Figure 34. Differences in maximum daily attic air temperatures recorded between three test attics using radiation control technologies and a baseline attic, during the June/July measure period.

Figure 34 shows clear superiority of the multifoil radiation control technology used in the attic 2A. For this attic, maximum air temperatures were, on average, about 8.5°C lower than the base case attic. It can be also observed that IRCC systems reduced maximum attic air temperature by over 6°C.

Following earlier analyses performed for the average attic temperature, a 8.5°C reduction of the maximum attic air temperature caused by the multifoil RB can be an equivalent to over 30% reduction of the attic-generated peak-hour cooling loads, considering maximum attic temperature of 53°C (as in Figure 29) and internal air temperature of 25°C.

Again, attic air temperature recorded in Unit 2A was the most different from the base case. Given the hotter temperatures in June, Unit 2B was typically the next most different attic temperature, as seen in Figure 34.

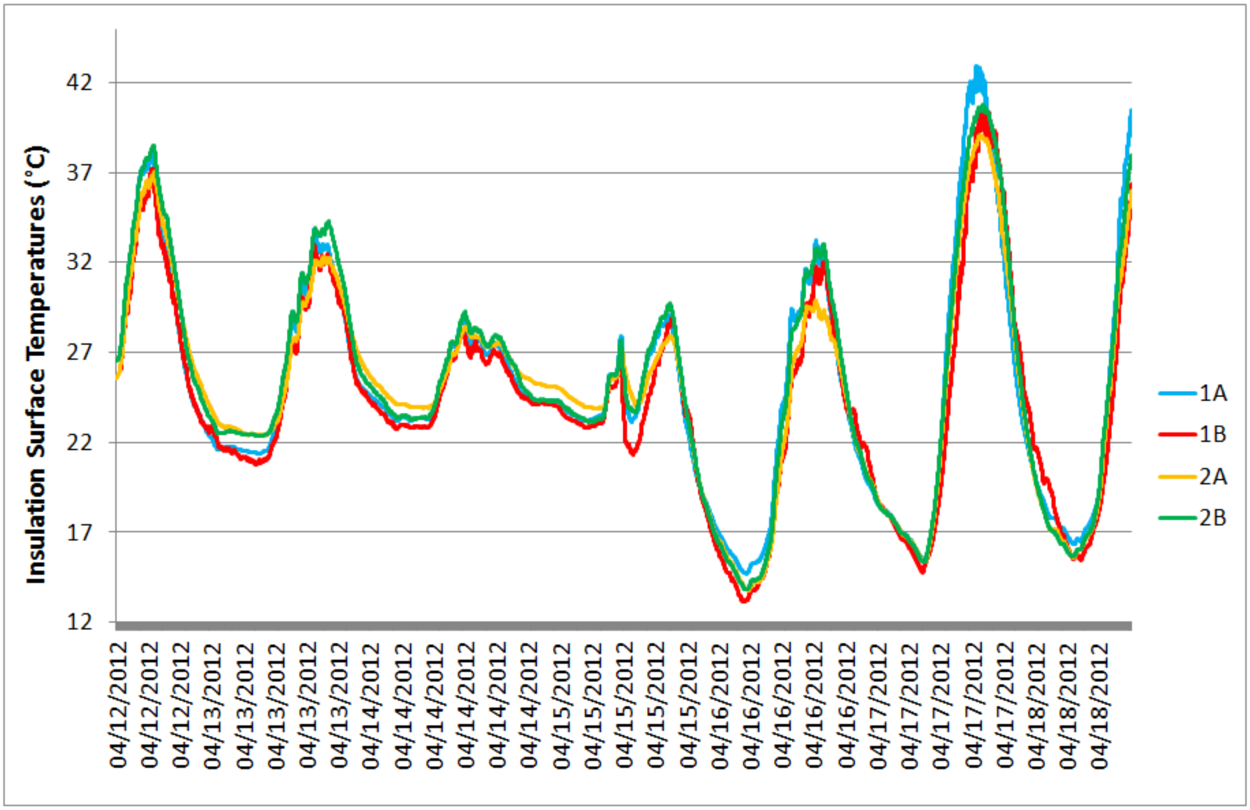

Figure 35. Daily temperatures on the top surface of the attic insulation recorded in four test attics using radiation control technologies and a conventional base case, during the April measure period.

The insulation surface temperatures were quite similar, as seen in Figure 35. Generally, the temperatures in Unit 2A were less extreme than for the other units. Maximum day temperatures were about 4°C lower than the conventional base case attic. In addition, 2A's attic stayed warmer during the night. The top of the insulation temperature was about 1°C warmer from all other attics. This was due to the additional thermal insulation of the two encased air cavities generated by the multifoils RB system; the first one between roof deck and aluminum foil and the second one between two foils.

In ideal conditions (when measurement perimeters were highly controlled and the insulation layer is uniform), temperature measurements on the top of the attic insulation could be a very good direct indicator of the technology thermal performance. However, in this experiment, due to the differences in construction, thicknesses of insulation and types of insulation in the individual attics, direct thermal performance comparisons were not possible using top insulation surface temperatures.

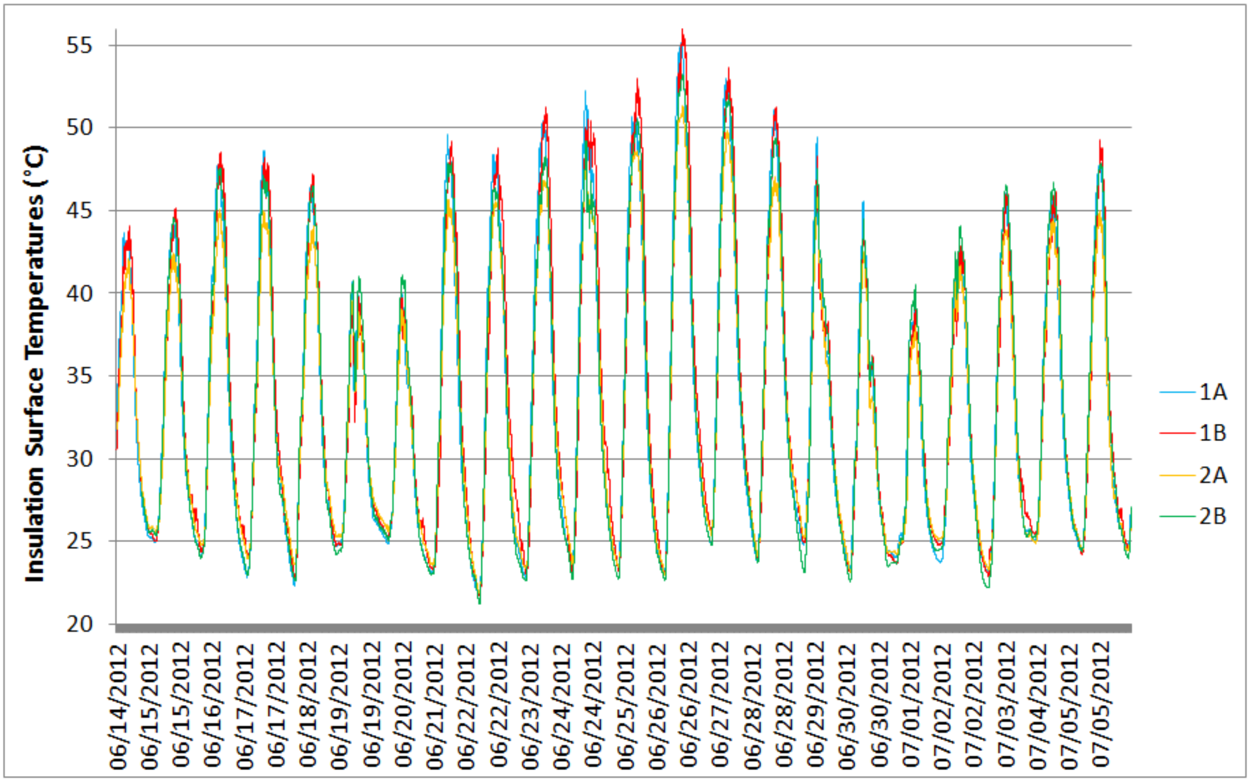

Figure 36. Daily temperatures on the top surface of the attic insulation recorded in three test attics using radiation control technologies and a conventional base case, during the June/July measure period.

In the hot month of June, the insulation surface temperatures were still quite similar. Again, Unit 2A appears to have less extreme temperatures, as shown in Figure 36. Maximum day temperatures on top of the attic insulation were about 4°C to 5°C lower comparing to the conventional base case attic. As mentioned earlier, these temperatures reflected the attic-generated peak hour cooling loads. Like April, during the night, the top of the insulation temperature stayed about 1°C warmer comparing to all other test attics. This fact made temperatures very close on average in all test attics, which may not have necessary reflected the relationships between attic generated peak-hour cooling loads (in contrast to daytime when insulation surface temperature is a good peak-hour thermal performance indicator).

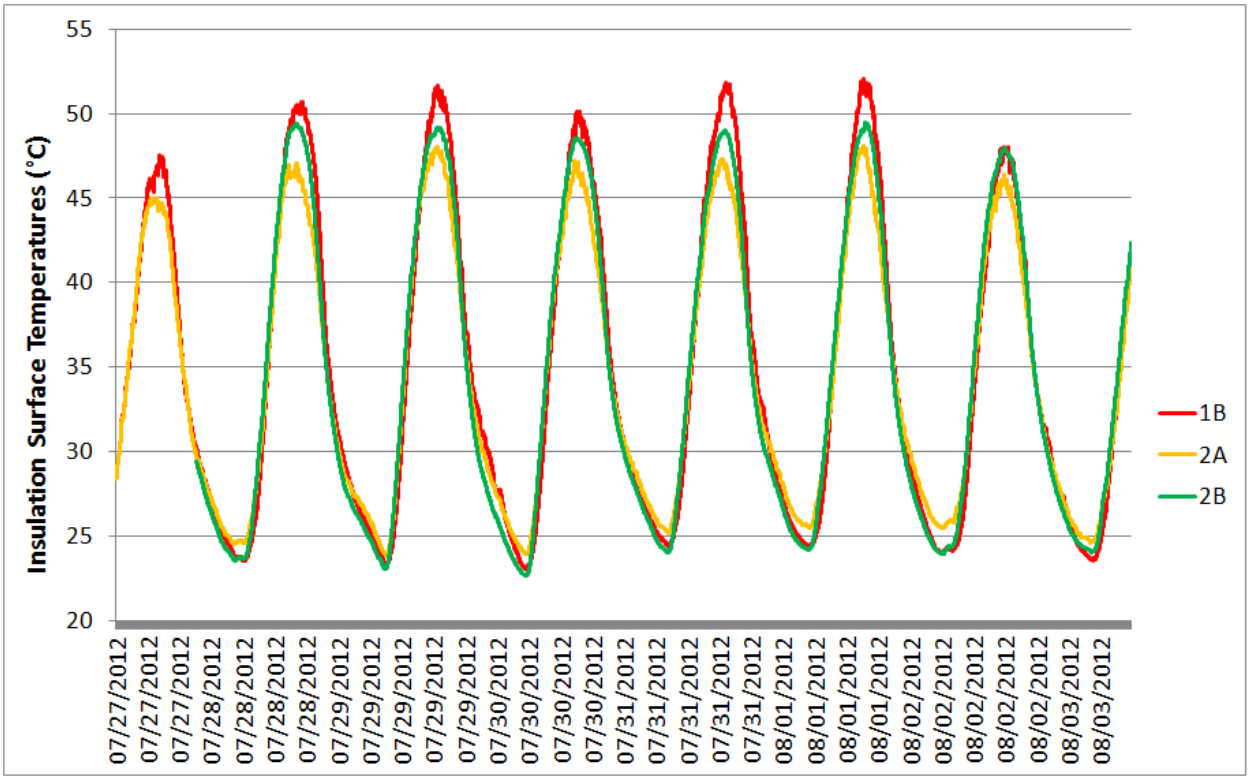

Figure 37. Daily temperatures on the top surface of the attic insulation recorded in two test attics using radiation control technologies and a conventional base case, during the July/August measure period.

In Figure 37, in the very hot month of July, Unit 2A appeared somewhat less extreme than 2B and 1B, which showed the greatest changes in temperatures. Still, maximum day temperatures on top of the attic insulation were about 4°C to 5°C lower comparing to other attics. During the night, top of the insulation temperature stayed about 1°C warmer in attic 2A, compared to all other test attics.

3.3 Experimental Heat Flux Comparison

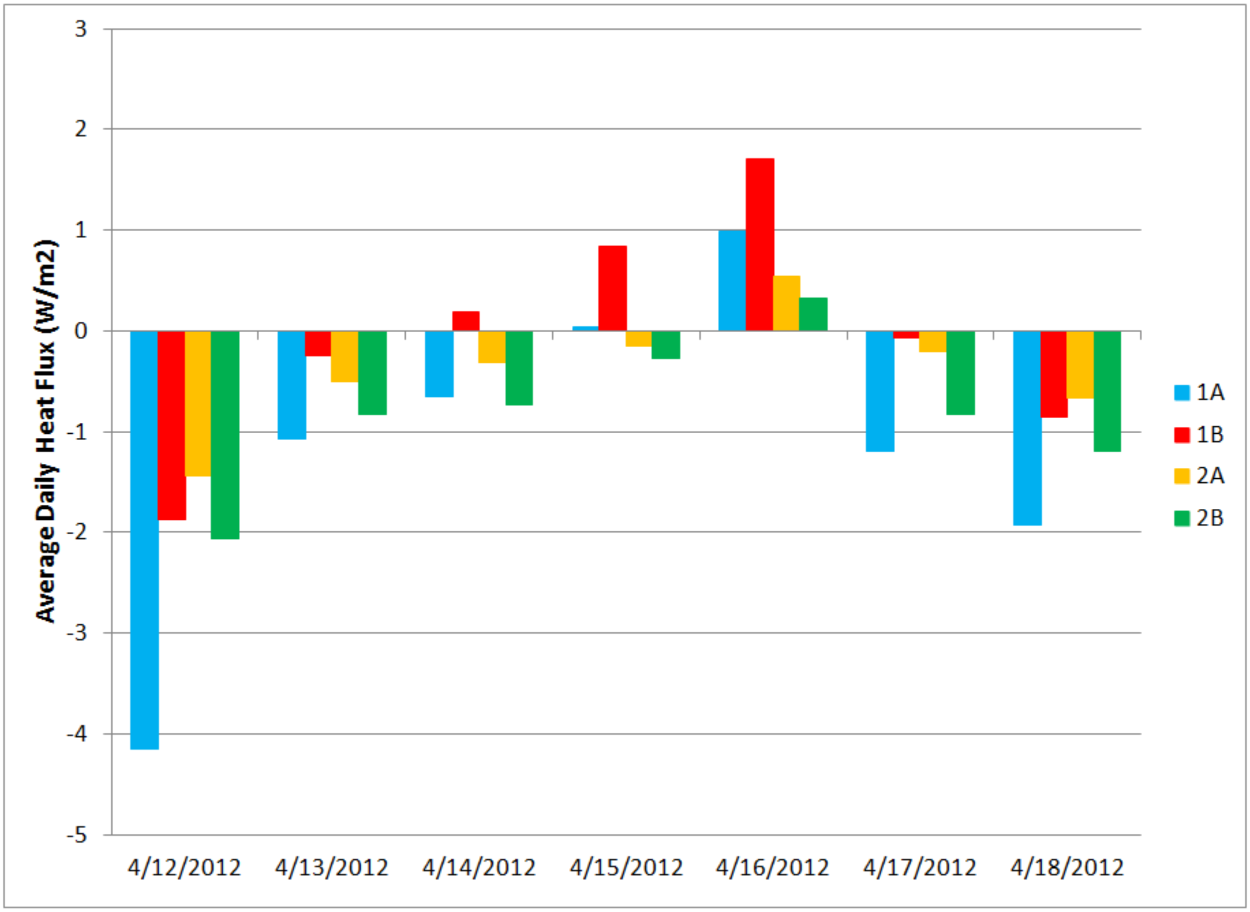

Figure 38. Heat fluxes recorded in four test attics using radiation control technologies and a conventional base case, during the April measure period. Positive heat flow direction is from conditioned space to the attic.

Because of different attic configurations and internal air temperatures, the heat fluxes measured on the ceiling level were not good indicators of performance compared to attic temperatures.

There were four factors that can affect this measurement: ventilation rates, R-values, internal temperatures, and air leakage through the attic ceiling. Figure 38 shows that the heat flux in 1A was typically larger than the other houses.

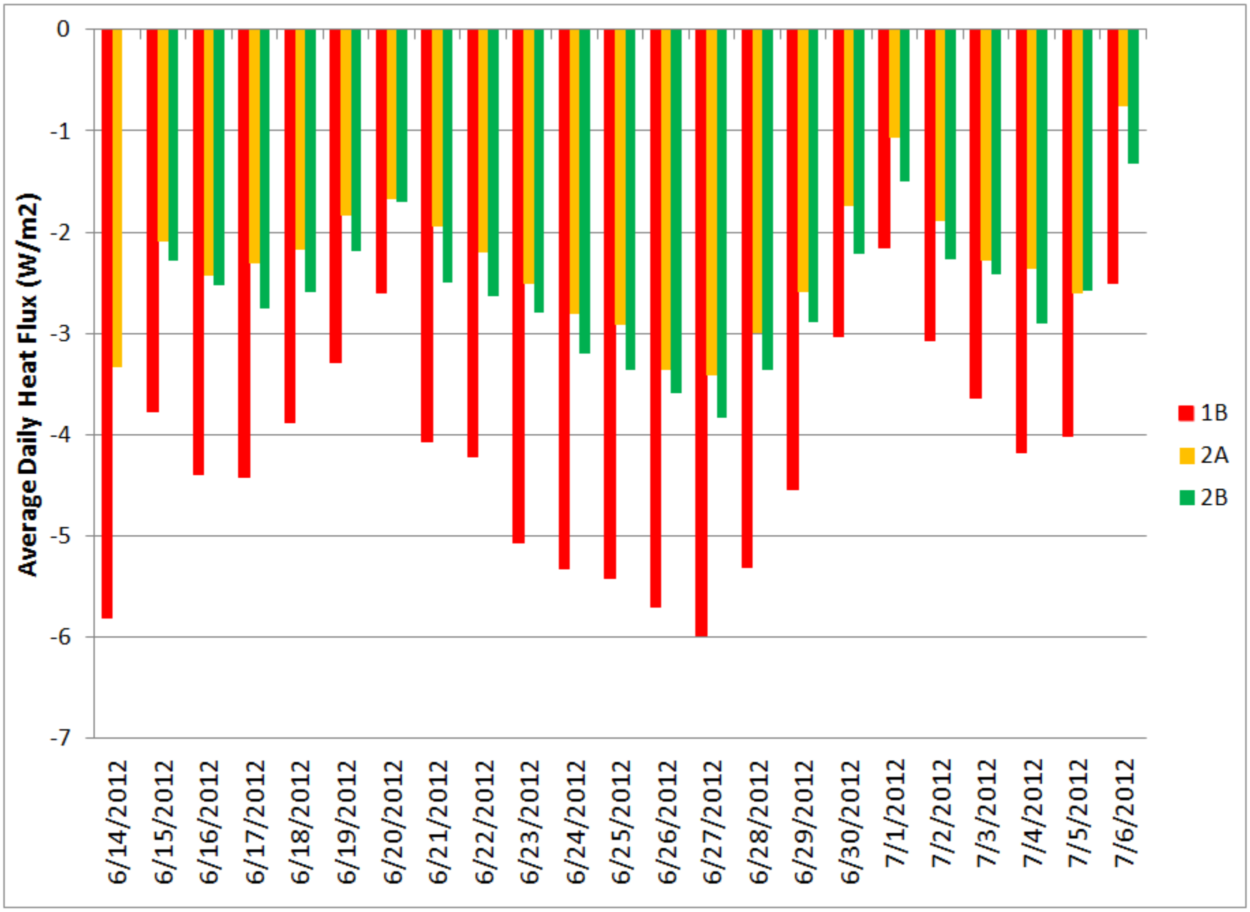

Figure 39. Heat fluxes recorded in test attics using radiation control technologies and a conventional base case, during the June/July measure period. Positive heat flow direction is from conditioned space to the attic.

In June, the measured heat flux in the house with IRCC technology was significantly higher than in the house with the foil technology, as seen in Figure 39. The largest differences are between units 2A and 2B. Heat fluxes measured in unit 2A were between 40% and 50% lower than heat fluxes measured for unit 1B.

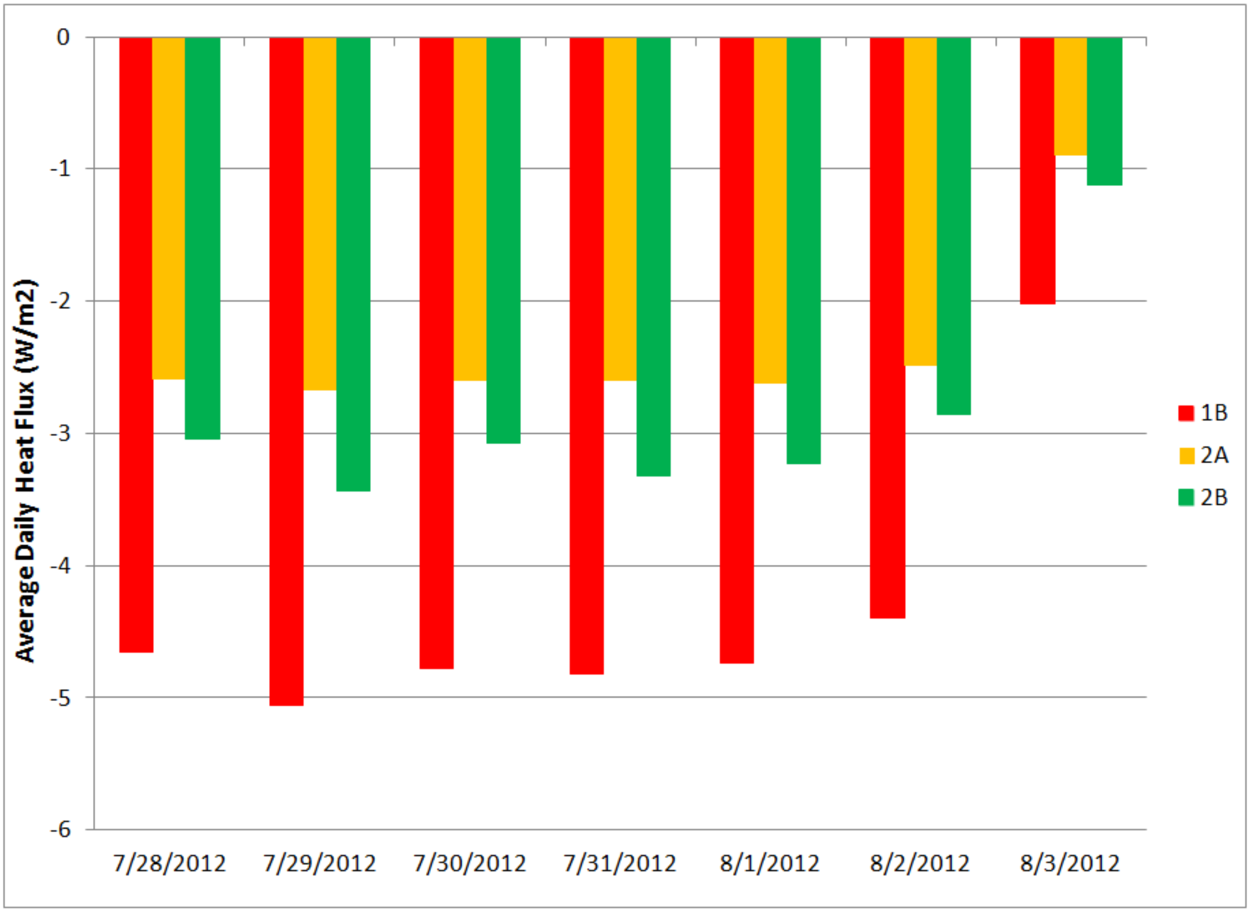

Figure 40. Heat fluxes recorded in test attics using radiation control technologies and a conventional base case, during the July/August measure period. Positive heat flow direction is from conditioned space to the attic.

Again, in July and August, the attic with the multifoil technology generated lower heat flux compared to the IRCC system unit 1B. This was a relatively large effect. Interestingly, heat fluxes measured on ceilings in the same Duplex 2 were within less than 20% difference only.

4 Energy Modeling

4.1 Model Description

The two duplexes in Austin were modeled using EnergyPlus 7.1 and SketchUp 8.0, with the Legacy OpenStudio Plug-in version 1.0.8 to generate the EnergyPlus input data files. The houses were each modeled as three zones representing the living space, attic, and garage (a total of six zones in each duplex). Other parameters are listed in Table 2.

Outside boundary conditions came from a weather file for Austin's climate. Wall and ceiling constructions were modeled in THERM to determine the effective thermal conductivity of the assembly layer containing the wood studs and insulation. As stated earlier, Duplex 1 was built between 1987–1997 and Duplex 2 was built prior to 1987. Compared to parameters listed in ASHRAE HOF Chapter 15, operable single-glazed windows with non-thermally broken aluminum frames, such as those installed in the duplexes, were confirmed. Solar heat gain coefficients were set to 0.79 in the model and U-factors were 0.92 Btu/h·ft^2·°F (5.2 W/m^2·K). Window construction was also kept consistent throughout the models.

Roofs were modeled as shingles and plywood with addition of the appropriate paint or foil layer where applicable. A no-mass material was specified in EnergyPlus to represent the IRCC and RB technologies. The absorptance of the material was lowered to decrease the amount of radiant transfer to other surfaces in the attic zone. Because of the non-uniform levels of insulation on the attic floor, an average value was calculated for use in the model. The team determined that both duplexes had approximate R-20, despite having different compositions—7.5 in. of loose cellulose in Duplex 1 while 3.5 in. of batt insulation plus an average of 3.5 in. of loose cellulose in Duplex 2, both with framing factors of 25%. Attic ventilation rates were estimated based on measurements of the area of attic vents in each of the test houses (Atherton, 2011).

Cooling setpoints were kept for modeling purposes at 76.1°F (24°C) for all four units. The heating setpoint was 68°F (20°C). Considering stratification of the temperatures, these temperatures were very close to that which was measured in 2012 in the test houses. However, it is important to notice that due to a change of some tenants followed by a possible change of space conditioning preferences, measured temperatures in two units were about 1°C higher from the other two. Two HVAC systems were added to each building, one per conditioned zone in each duplex. The Unitary Template in EnergyPlus was used to model the forced air system with a 2.5 rated coefficient of performance (COP) single-speed direct expansion cooling coil and natural gas heating coil with an efficiency of 70%. Considering the losses due to duct leakage and the condenser unit, the overall COP of the system was reduced in the model from the manufacturer's COP. The natural gas water heater had a thermal efficiency of 80%. The models were calibrated against gas consumption data obtained from utility bills during winter. The maximum hot water flow was obtained through calibration of gas consumption with the amount reported by Texas Gas Service calculator for a typical residential single family house in Austin.

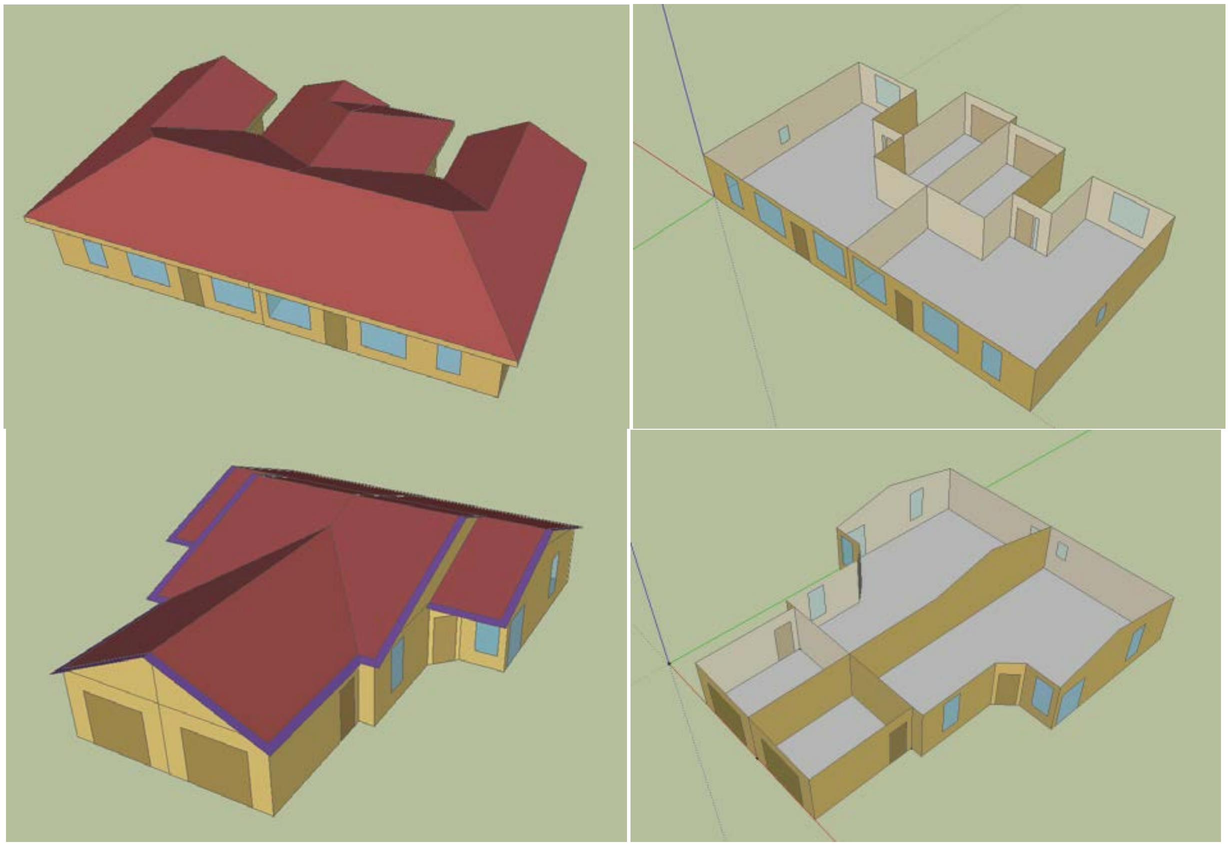

Figure 41. Duplex 1 model (above); Duplex 2 model (below).

Table 2. Model Parameters.

Model Parameters			Duplex 1		Duplex 2	
			Unit A (Baseline)	***Unit B (IRCC)***	***Unit A (RB)***	***Unit B (IRCC)***
Zones			3; Attic, Living, Garage	3; Attic, Living, Garage	3; Attic, Living, Garage	3; Attic, Living, Garage
Infiltration (ACH)	*Attic*		10	10	10	10
	Living		1.2	1.2	1.2	1.2
	Garage		1.2	1.2	1.2	1.2
Construction	*Wall assembly*		Siding, Plywood, 2x4 wood studs with semi-rigid insulation, Gypsum	Siding, Plywood 2x4 wood studs with semi-rigid insulation, Gypsum	Siding, Plywood 2x4 wood studs with semi-rigid insulation, Gypsum	Siding, Plywood 2x4 wood studs with semi-rigid insulation, Gypsum
	Wall R-Value (whole assembly)		10	10	10	10
	Roof assembly		Shingle, Plywood	Shingle, Plywood, IRCC (LO/MIT;ε=0.17)	Shingle, Plywood RB (Fi-Foil; ε =0.03)	Shingle, Plywood, IRCC (HeatBloc-Ultra; ε= 0.19)
	Ceiling R-value (whole assembly)		20.2	20.2	20.2	20.2
	Attic Framing Factor		0.25	0.25	0.25	0.25
	Window type		Single glazing	Single glazing	Single glazing	Single glazing
	Glazing Ratio	*North*	14.01%	14.01%	2.80%	2.80%
		South	31.30%	31.30%	9.51%	9.51%
		East/ West	1.90%	1.90%	12.32%	12.32%
	Window U-Factor (Btu/h·ft^2·°F)		0.92	0.92	0.92	0.92
	Window SHGC		0.79	0.79	0.79	0.79
HVAC Setpoints (°F)	*Cool*		75.2	75.2	75.2	75.2
	Heat		68	68	68	68
People			2.5	2.5	2.5	2.5
Lighting (W)			1100	1100	1100	1100
Electrical Equipment (W/ft2)			0.46	0.46	0.46	0.46
Water Heater Thermal Eff.			0.8	0.8	0.8	0.8

4.2 Calibration of Whole Building Energy Model

In order to predict energy consumption of the duplexes with reliable accuracy, the EnergyPlus models were calibrated against historical utility bills obtained for tested houses. For this purpose, the computer-generated energy consumptions were compared with historical energy bills for both heating and cooling seasons.

It is important to mention that, due to complexity of the test attics and the fact that buildings were occupied during the testing, it was impossible to validate the thermal simulation algorithm used for attics by EnergyPlus. Therefore, EnergyPlus simulation results (cooling energy savings) presented in this study need to be confirmed in the future either by more accurate computer models (like ATTICSIM–ASTM C1340) or by calorimetric field measurements with use of the test huts. Additionally, due to limited amount of available historical bill data, the comparison was done only for duplex 1B.

During the heating season, the main sources of energy consumption were a furnace for space heating and a water heater for domestic hot water. Based on Texas Gas Service's home energy calculator, for a typical single family house with similar characteristics to the test houses, close to 50% of total gas consumption was space heating, approximately 35% water heating and 15% was cooking, as shown in Figure 42. Therefore, to capture these main sources of gas consumption, a water heater, furnace and gas equipment were considered in the model. Figure 43 compares the simulated gas consumption with historical energy bill and Texas Gas Service for duplex 1B. There was a relatively good agreement between EnergyPlus-generated gas consumption and historical gas service data. Note that EnergyPlus used the actual weather file which is the observed weather data for the duration of the modeling. Figure 43(a) and 43(b) compare gas consumption of duplex 1B with historical gas bill before and after applying the radiation technology, respectively. The data confirms proper selection of the building enclosure and HVAC system parameters for whole building energy consumption simulations.

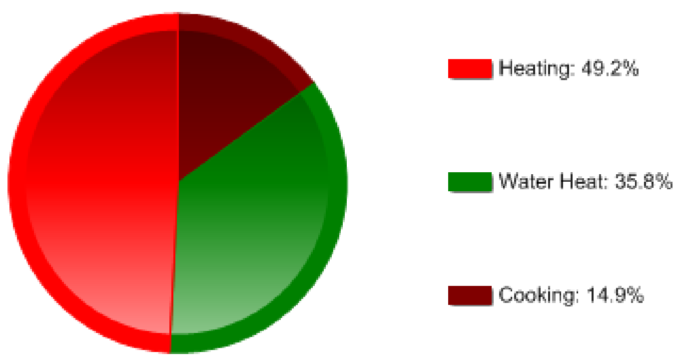

Figure 42. Breakdown of household gas consumption.

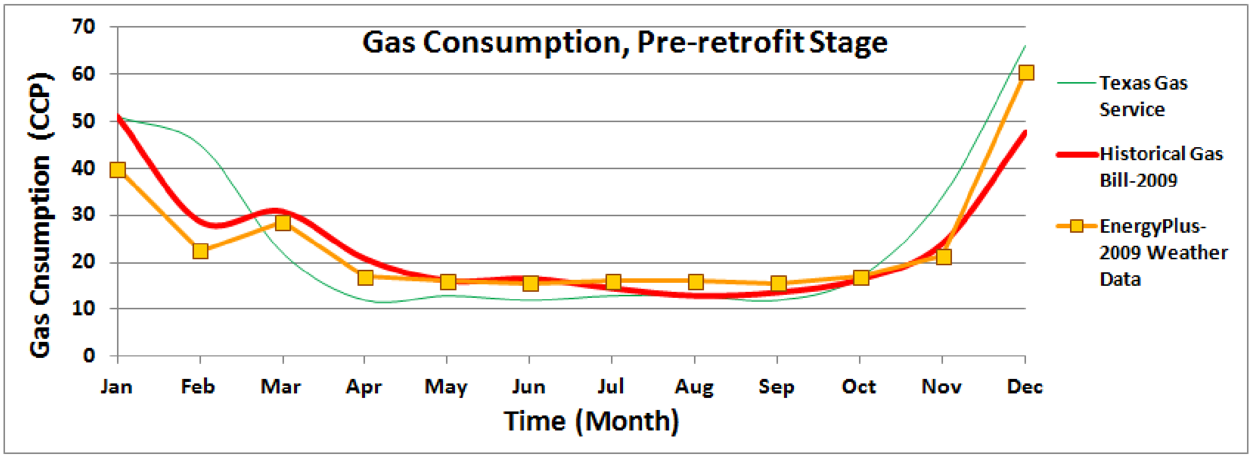

a) Gas consumption of duplex 1B before installing radiation control technology. The EnergyPlus simulation is based on actual weather file data from 2009.

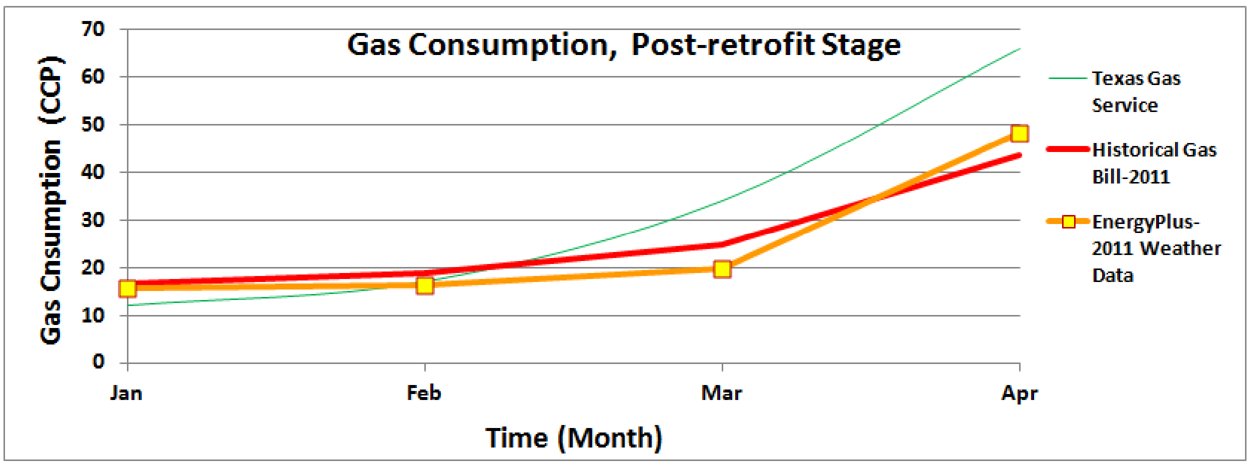

b) Gas consumption of duplex 1B before installing radiation control technology. The EnergyPlus simulation is based on the observed weather data file from 2011.

Figure 43. Comparison of monthly historical gas bill, simulated consumption, and the gas consumption by Texas Gas Service calculator. The calibration is limited to the months with available historical utility bill.

Using the actual weather data file enabled comparisons to energy consumption results generated with a use of the Texas Gas Service's home energy calculator[5]. During the cooling season, the main sources of electricity consumption were AC unit for space cooling, lighting and appliances. Again, referring to Texas Gas Service's home energy calculator in Figure 44, for a typical single family house, close to 80% of total electricity consumption was for space cooling, 8.5% for lighting and close to 11.5% for appliances and others.

[5] http://www.texasgasservice.com/SaveEnergyAndMoney/HomeEnergyCalculator.aspx

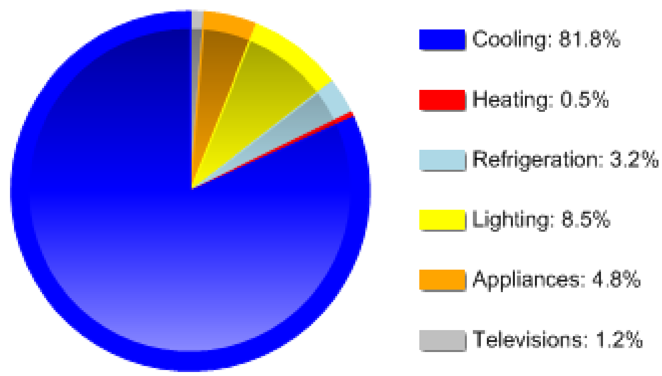

Figure 44..Breakdown of household electrical consumption.

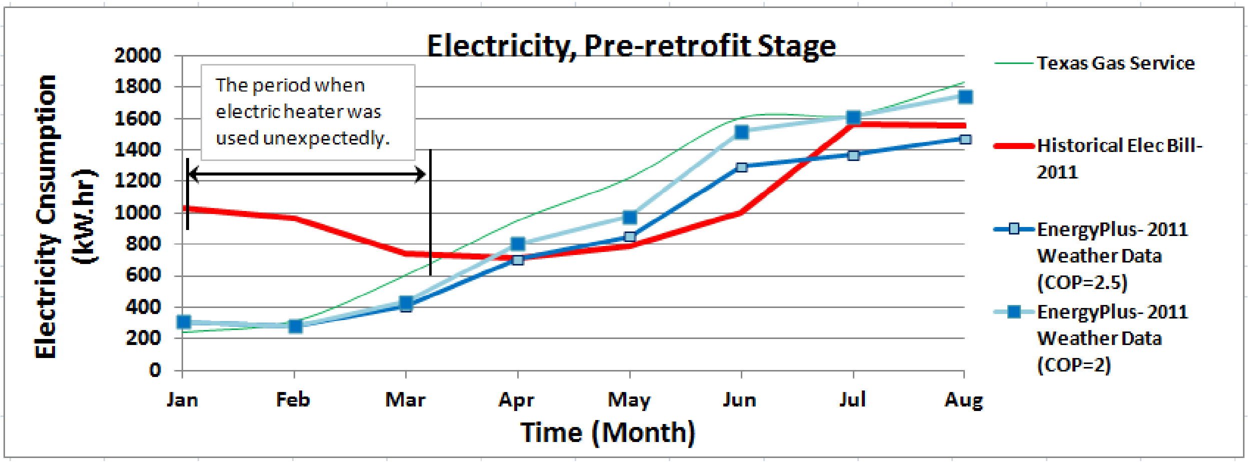

a) Electricity consumption of Duplex 1B before installing radiation control technology. The EnergyPlus simulation is based on actual weather data file from 2011. High electricity consumption during heating season is due to unexpected usage of the electric heater by the tenants. A cooling system with COP=2.5 was considered throughout this report; however, as a parametric study, cooling system with COP=2 was modeled and compared in this graph.

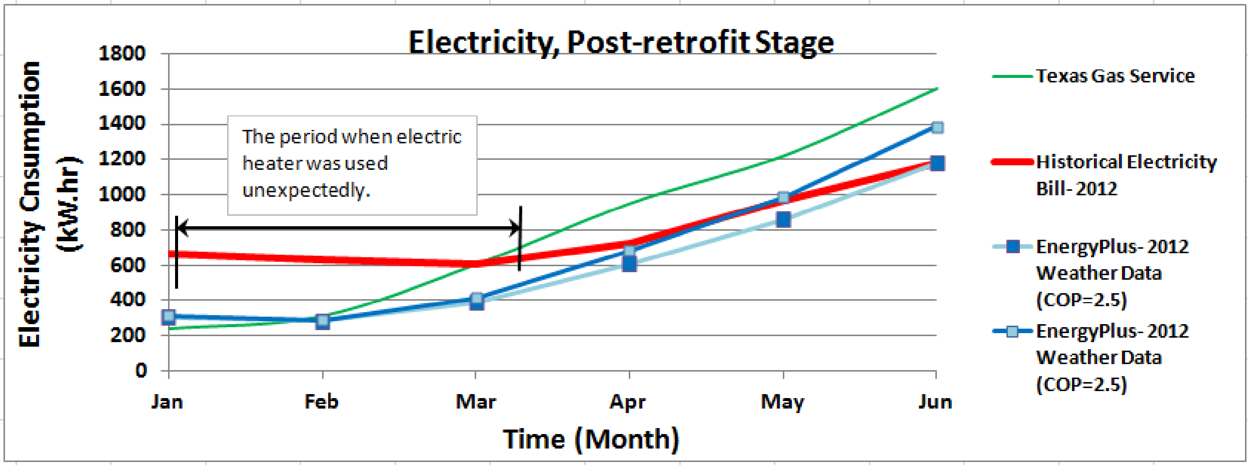

b) Electricity consumption of Duplex 1B after installing the radiation control technology. The EnergyPlus simulation is based on actual weather data file from 2012. High electricity consumption during heating season is due to unexpected usage of electric heater by the tenants. A cooling system with COP=2.5 was considered throughout this report; however, as a parametric study, cooling system with COP=2 was modeled and compared in this graph.

Figure 45. Comparison of monthly historical electricity bill, simulated consumption, and the electricity consumption by Texas Gas Service calculator. The calibration is limited to the months with available historical utility bill.

As Figure 45 shows, EnergyPlus predicted well the electricity consumption during the cooling season compared with historical electricity bill and Texas Gas Service's calculator. However, during the heating season, there were discrepancies due to the fact that the test houses were using auxiliary electricity for heating. Overall, considering the fact that the historical electricity bill was not prorated and both the AC unit set point and consumer behavior were approximated, the prediction of energy consumption particularly during the cooling season seemed in good agreement with historical bills and Texas Gas Service's calculator.

4.3 Prediction of the Cooling Energy Consumption

As described, the models' calibration was based on comparison between electricity and gas consumption data with simulated energy use in the models with historical data from the Texas Gas Service calculator. The calibrated models were simulated with a TMY3 weather file for Austin Mueller Municipal Airport to predict the electricity consumed by AC units during cooling season.

4.4 Modeling Results

In the summer, a higher infiltration rate of the attic reduced the attic temperature by exchanging the outdoor air with the attic air that was heated by the roof. The lower attic temperature reduced the heat flux through the ceiling of the living space. The wall construction and infiltration rate of the living space also affected the cooling load placed on the HVAC system. Finetuning the RB was required to model the emissivity within the attic space accurately and the thermal conductivity through the layer, and in the case of the Fi-foil, the air gap between the roof and the RB.

The results from EnergyPlus using a typical meteorological year (TMY3) indicate that the energy consumption is well below the range approximated based on the measurements performed during the experiment. In addition, EnergyPlus-generated cooling energy savings are at least five times lower than the earlier findings from different U.S. research studies summarized (Medina, 2012).

Table 3. Predicted Energy cooling Consumption and Associated Savings from Radiation Control Technologies.

Cooling Energy Consumption / Test Unit	Without Radiation Control Technology	With Radiation Control Technology	Annual Cooling Energy Savings
1A (Baseline)	4333 kWh	N/A	N/A
1B (IRCC)	4326 kWh	4308 kWh	0.43%
2A (RB)	4703 kWh	4703 kWh	1.27%
2B (IRCC)	4922 kWh	4922 kWh	0.83%

The modeling results in Table 3 show that cooling energy is saved with the use of radiation control technologies. The table lists and compares the modeled annual cooling energy consumption of each house before and after implementing the radiation control technology. The "Annual Cooling Energy Savings" for each house in Table 3 is calculated by comparing cooling energy consumption in "Without Radiation Control Technology" and "With Radiation Control Technology" columns. The Fi-Foil shows the highest savings from its lower emissivity and the air gap created between the roof and the space between the two layers of the foil. Comparing the two duplexes with IRCC installed, the results show that the attic geometry and the amount of roof coated with the low-e material make a difference in the performance.

Parametric studies of the convection coefficients, air exchange rate, set point temperature and changes of the heat transfer rate through exterior walls and windows were performed in the process of calibrating the model. Convection coefficients were specified from the ASHRAE Handbook of Fundamentals. The values for horizontal down flow were used and a slight improvement was expected from the values EnergyPlus calculated. This was expected since all roof surfaces were at angles above horizontal. The air exchange rate made little difference in the output of the model. This is likely because the exchange of air has a greater effect on the zone air temperature than the surfaces temperatures, which govern radiant heat flow. Heat flow through the exterior walls and windows had the greatest effect on the performance of the RB since heat flow through the ceiling into the conditioned zone was proportionally less than the other surfaces even though the heat flux through the ceiling remained the same.

It should be noted that the above savings have been estimated based on EnergyPlus modeling parameters close to existing test house conditions. Depending on HVAC configuration, air leakage rate, and building envelope parameters, the savings can increase close to twice the values reported in Table 3. However, they will still be significantly lower than the results of earlier experimental studies (Medina 2012). This is one of the most surprising findings from this study.

Recorded temperature and energy consumption data showed that one test unit was notably different during the winter 2011, which was evidence of an extensive use of an electric heater. The use of a supplemental heater was unexpected, and an electric heater was not instrumented. An additional challenge in modeling was caused by the fact that the tenant changed in one of the test units just before the start of measurements. Also, the inability to control setpoint differences between the units made direct comparisons difficult (since test units were occupied by tenants with various space conditioning preferences).

One of the conclusions from this study is the fact that it is extremely difficult to conduct a detailed performance analysis of a single building enclosure system like RB using field test data from occupied vintage housing units. It is still unclear how well energy consumption predictions of the building systems containing RBs can be simulated using simplified Energy Plus roof/attic algorithm. The team recommends that in the future, a calorimetric type of a field experiment (with precisely measured attic air leakage rates, level of attic insulation, and with simple attic structural components) be performed in order to further validate EnergyPlus predictions in cases of RB applications. This experiment will most likely require test huts or similar small and well-instrumented test structures.

5 Cost Effectiveness Analysis

For the purpose of cost analysis, a range of cooling load savings achievable by applying RB and IRCC was assumed. The upper limit of this saving range was obtained from the available review of earlier research studies provided (Medina, 2012). Taking R-19 (hr·ft²·°F/Btu) attic insulation as a baseline, according to published literatures (Medina, 2012, Stovall et al., 2010), the team found that approximately 20% and 14% cooling load saving can be achieved by applying RB and IRCC technologies underside of attic roof, respectively. Similarly 4% and 2.4%[6] heating load saving is possible for RB and IRCC technologies. At some point, these numbers can be questioned, considering that in most of the U.S. residential houses, attic-generated cooling loads represent approximately 12% of the whole building loads (Huang et al., 1996). That is why the lower limit of savings representing 20% of the upper limit was assumed in this study as well. This 20% lower limit was chosen since it yields a 4% cooling load reduction for RB, a similar level as the cooling energy savings calculated from measured data analysis (see Chapter 3).

In this analysis, the developed EnergyPlus models were used to simulate the energy performance of a single-family residence as a baseline house in representative U.S. climates. The same single story house was used for development of Model Energy Code (Council of American Building Officials, 1995) and ASHRAE 90.2 (ASHRARE 2007).

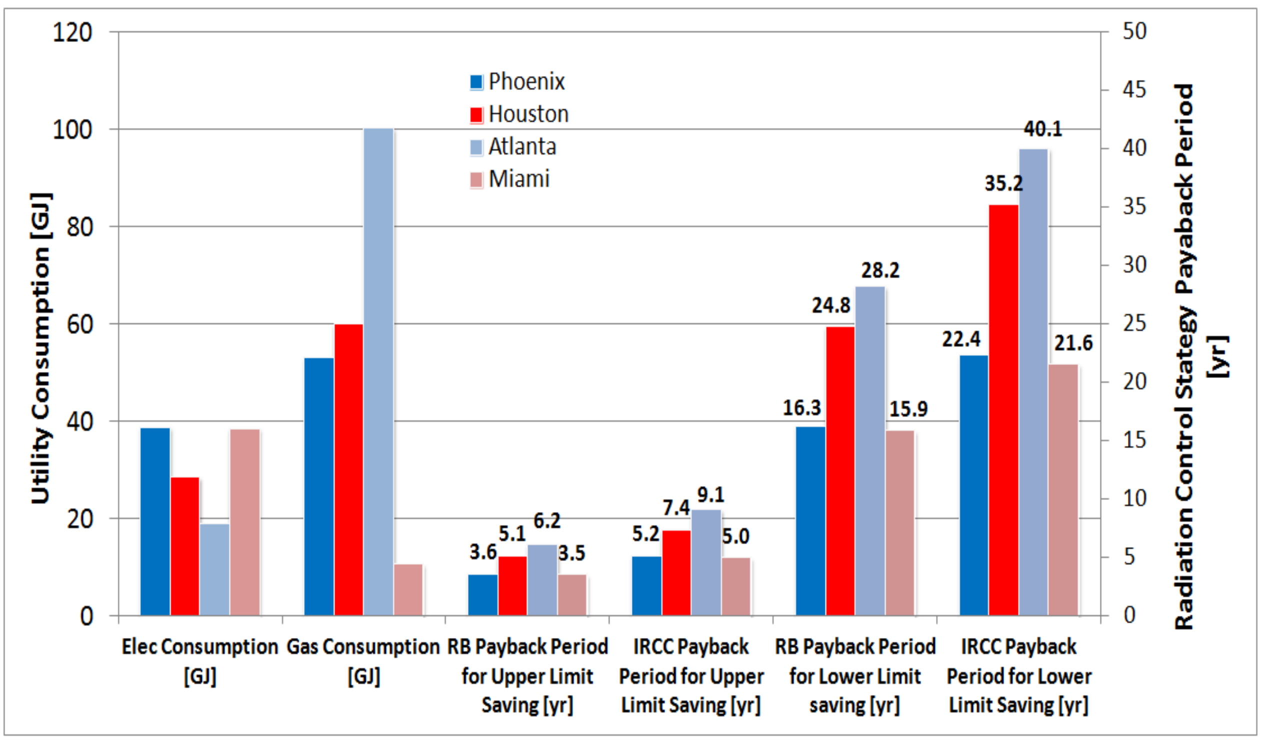

Figure 46. Modeled utility consumption of baseline house in different U.S. South climates and payback period of radiation control strategies.

The simulations were performed for four U.S. climates using weather files. The energy performance of this baseline house is presented as utility consumption rate (electricity and gas).

[6] Based on Medina (2010), IRCC heating load saving estimated to be 61% of RB heating load saving

To evaluate the payback period, the heating and cooling loads were modeled for the baseline house with R-19 attic using EnergyPlus. Having these modeled loads, the radiation control strategies load savings suggested by literature (upper limit for the energy savings of 20%, 14% summer savings, and 4% and 2.4% winter savings for RB and IRCC, respectively, according to Medina 2012; and lower limit of 20% of the above savings) were calculated, as well as the associated consumptions rate and energy cost savings. It is important to mention that the calculated 20% cooling energy savings level (of the data presented in literature—see Medina 2012) was close to energy savings approximated based on the results of this field study. The payback periods were estimated by comparing the cost savings and the installed cost[7] of RB and IRCC in the attic.

It should be noted that both RB and IRCC contractors provided the same quoting prices for their installed products ($0.75 per square foot). Following direct observations performed during the installation process, the above cost numbers seem unreasonable due to the fact that not only the material usage but also the labor costs were notably different for each of the considered technologies. As an example of a similar installation process, the labor cost of painting work and air barrier installation work are significantly different according to RS MEANS 2011. Therefore, although the payback period has been shown in Figure 46, it should be highlighted that the calculations are based on the same quoting price value received from RB and IRCC contractors.

As shown in Figure 46, the climate with higher electricity consumption or higher cooling loads has shorter payback period since the radiation control strategies provided more savings in cooling rather heating season.

Table 4. Residential Utility Price Based on Considered Climates.

Climate	Elec. Price[8] [$/kW.h]	Gas Price[9] [$/THERM]
Phoenix	0.110	1.31
Houston	0.107	0.79
Atlanta	0.102	1.24
Miami	0.122	1.49

[7] The installed cost based on contractors quotes.
[8] Edison Electric Institute Typical Bills and Average Rates Report, January 2011
9 Department of Energy for monthly “bundled” supply and delivery costs for January 2011

6 Conclusions

The major goal of this project was to evaluate the energy effects of RBs and IRCCs in field conditions. Major focus was paid on thermal and energy performance of the attics. During the cooling season 2012, thermal performance measurements were performed on four housing units in two residential duplexes. Three test attics were modified using RBs and IRCCs and tested, while the fourth attic stayed unmodified and was used as a base case for comparisons.

Two main goals of this report were thermal performance analysis and cost comparisons of three radiation-control technologies used in the field testing. Thermal performance data was collected during three time periods of April, June/July, and July/August 2012. Field experiments took place in Austin, Texas. All test houses were occupied during the testing by residents. The original plan was to keep internal load schedules in the test units as close as possible; however, each of these tenants had different occupation habits and thermal comfort preferences. Also, individual schedules for operating the AC were different. In addition, the test houses had attics with varying structural components, thicknesses and types of attic floor insulation, and levels of attic ventilation. All of the above factors made direct comparison of the whole building energy consumption impossible.

Measured test data confirmed earlier results from other research organizations. An average 3.4°C reduction of the average attic air temperature caused by the multifoil RB was recorded during mid-summer 2012, and can be equivalent to over 34% reduction of the attic-generated cooling loads—assuming approximate steady-state heat transfer, average attic temperature of 35°C (as in Fig. 12) and internal air tmperature of 25°C. This is consistent with a range of the cooling load reductions reported by Medina (2012). It has been also reported that for U.S. residential houses, roofs and attics generate an average 12% cooling energy contributions (Huang, et al., 1996). In that light, potential whole building cooling energy savings may reach about 4%, depending on other building parameters and HVAC system efficiency.

Similarly, a 2.4°C reduction of the average attic air temparature caused by the IRCC technology can be an equivalent to over 24% reduction of the attic-generated cooling loads, and potential whole building cooling energy savings for this technology may be close to 3%. Based on the recorded data, energy performance of two IRCC systems seems to be very similar considering the small differences in construction of both test attics in Duplexes 1 and 2.

An EnergyPlus computer model calibrated against both gas and electricity historical bill data for the periods of pre-retrofit and post-retroft was used for prediction of potential cooling energy savings. The results from EnergyPlus were well below the range of cooling energy savings approximated based on the measurements performed during this experiment. In addition, EnergyPlus-generated cooling energy savings were at least four to five times lower than results available from the earlier studies (Medina, 2012). The team recommends more work on validation of whole building computer models using attic algorithms with RB.

For the purpose of cost analysis, each of the reflective insulation companies participating in the project were asked for cost estimates based on the records from installation of their technologies in the test houses. Surprisingly, cost data provided by RB and IRCC companies had similar prices per square foot of the installed radiation control system in the attic. These uniform costs were used in the following payback time calculations; however, in the future, they should be confirmed in additional projects.

To evaluate the payback period, the heating and cooling loads were modeled for the baseline house with R-19 attic insulation using EnergyPlus. With these modeled loads, the radiation control strategies load savings suggested by literature was calculated, as well as the associated consumptions rate and energy cost savings. This is based on 20% and 14% summer savings, and 4% and 2.4% winter savings for RB and IRCC, respectively, according to Medina 2012; and 20% of the above savings, which yields 4% and 2.8% cooling energy savings—close to the results of this field study. The payback periods were estimated by comparing the cost savings and the installed cost[10] of RB and IRCC in the attic. Four southern U.S. locations were used for this analysis. When higher energy savings (according to Medina 2012) are considered, RB and IRCC systems yielded the lowest payback times for Miami, FL and Phoenix, AZ—about 3.5 years and 5 years, respectively. When savings levels were similar to results recorded during this experiment are considered, the payback times for the same locations are 16 and 22 years, respectively for RBs and IRCCs.

10 The installed cost based on contractors quotes.

References

CABO (1995). Model Energy Code; 1995 Edition. Falls Church, Virginia: Council of American Building Officials.

ANSI/*ASHRAE 90.2*-2007: Energy Efficient Design of Low-Rise Residential Buildings

ASTM Standard C1313. (2010). "Standard Specification for Sheet Radiant Barriers for Building Construction Applications". ASTM International, West Conshohocken, PA, DOI: 10.1520/C1313_C1313M-10.

ASTM Standard C1340. (2010). "Standard Practice for Estimation of Heat Gain or Loss Through Ceilings Under Attics Containing Radiant Barriers by Use of a Computer Program". ASTM International, West Conshohocken, PA, DOI: 10.1520/C1340_C1340M-10.

ASTM Standard C1321. (2009). "Standard Practice for Installation and Use of Interior Radiation Control Coating Systems (IRCCS) in Building Construction". ASTM International, West Conshohocken, PA, DOI: 10.1520/C1321-09.

Atherton, S.A. (2011). "Residential Attic Ventilation In A Hot And Humid Climate: Effects Of Increased Ventilation On Thermal Performance and Moisture Control", Master Thesis, University of Tennessee, Knoxville.

DEG. (2000). "Simulated Attic Radiant Barrier Performance in Six U.S. Locations". Davis Energy Group, Inc., Davis, CA.

DOE (various dates). Building America - Resources for Energy Efficient Homes. U.S. Department of Energy. Accessed at: www.buildingamerica.gov. .

DOE (2012). Residential Natural Gas Average Monthly State Costs, Bundled Service – Supply and Delivery Costs – As of July 2012. . U.S. Department of Energy. Accessed at: http://www.northwesternenergy.com/ourcustomers/shared/NaturalGasRates.pdf

Edison Electric Institute (2012). Residential Electric Monthly Costs – July 2012 750 kWH Bundled Service – Supply & Delivery Costs Accessed at: http://www.northwesternenergy.com/ourcustomers/shared/ElectricRates.pdf

Fifoil products technical data sheet. Available at: http://www.fifoil.com/Builders/Products/ProductInfo/?ID=3.

Hancock, E., Norton, P., and Hendron, B. (2002). "Building America System Performance Test Practices: Part 2, Air Exchange Measurements" NREL Technical Report NREL/TP-550-30270. Accessed at: http://www.nrel.gov/docs/fy02osti/30270.pdf

Huang, J., Hanford, J. and Yang, F. (1996). "Residential Heating and Cooling Loads Component Analysis.". LBNL Technical Report LBNL-44636. Accessed at: http://simulationresearch.lbl.gov/dirpubs/44636.pdf.

Lenntech (2010). "Aluminum". Available at: http://www.lenntech.com/periodic/elements/al.htm

Medina, M. (2012) "A Comprehensive Review of Radiant Barrier Research Including Laboratory and Field Experiments", ASHRAE Transactions; 2012, Vol. 118 Issue 1, p400 http://blog.radiantbarrier.com/wp-content/uploads/2012/02/radiant-barrier-research-ashrae.pdf.

Parker, D. S. (2005). "Literature Review of the Impact and Need for Attic Ventilation in Florida Homes". Florida Solar Energy Center Report FSEC-CR-1496-05. Accessed at: http://www.fsec.ucf.edu/en/publications/pdf/FSEC-CR-1496-05.pdf.

Parker, D. S. (2003). "Research highlights from a large scale residential monitoring study in a hot climate". *Energy and Buildings*. 35 (9), pp. 863-87.

Parker, D. and Sherwin, J. (1998). "Comparative Summer Attic Thermal Performance of Six Roof Constructions", *Proceedings of the 1998 ASHRAE Annual Meeting*, Toronto, Canada.

RIMA International (2002). "Understanding and Using Reflective Insulation, Radiant Barriers and Radiation Control Coating". Second Edition. Accessed at: http://www.rimainternational.org/pdf/handbook.pdf.

RS Means Building Construction Cost data (2011). http://rsmeans.reedconstructiondata.com/

Stovall, T., Yarbrough D. W., Shrestha S., Pearson T. and Arimilli R. V. (2010). "Analysis in Support of the Radiant Barrier Fact Sheet 2010 Update". Proceedings of Thermal Performance of Exterior Envelopes of Whole Buildings XI , Florida. Accessed at: http://web.ornl.gov/sci/buildings/2012/B11%20papers/141_Stovall.pdf .

Texas Gas Service, Home Energy Calculator. Available at: http://www.texasgasservice.com/en/SaveEnergyAndMoney/HomeEnergyCalculator.aspx

Wallace, L.A., Emmerich, S.J., and Howard-Reed, C. (2002)."Continuous measurement of air change rates in an occupied house for 1 year: the effect of temperature, wind, fan and windows." 2002. Journal of Exposure Analysis and Environmental Epidemiology (12) pp. 296- 306.

Appendix A- Historical Energy Consumption Data

Utility data from the four units was made available. This was useful for comparing against monthly consumption results from the simulations. The model was calibrated against Unit 1B's electricity data from November 2010-November 2011 and gas data from 2009.

Duplex 1, Unit B

Gas		
Date	***Usage (ccf)***	***Billed***
26-Jan-09	51	$66.87
24-Feb-09	28	$37.24
25-Mar-09	33	$40.01
24-Apr-09	22	$26.09
26-May-09	16	$19.32
24-Jun-09	17	$19.90
24-Jul-09	15	$20.65
24-Aug-09	13	$18.97
23-Sep-09	13	$17.87
26-Oct-09	16	$21.44
23-Nov-09	19	$24.96
22-Dec-09	41	$41.60
24-Jan-11	49	$45.08
23-Feb-11	58	$51.51
24-Mar-11	29	$32.31
22-Apr-11	23	$28.11

Duplex 1, Unit B

Electric		
Date	***Usage (kWh)***	***Billed***
11-Jan	1036	$89.93
11-Feb	970	$83.79
11-Mar	737	$62.12
11-Apr	709	$59.51
11-May	792	$72.55
11-Jun	1001	$95.78
11-Jul	1563	$158.26
11-Aug	1560	$157.92
12-Jan	664	-
12-Feb	631	-
12-Mar	603	-
12-Apr	720	-
12-May	968	-
12-Jun	1177	-

buildingamerica.gov

U.S. DEPARTMENT OF ENERGY | Energy Efficiency & Renewable Energy

DOE/GO-102013-3943 ▪ December 2013

Printed with a renewable-source ink on paper containing at least 50% wastepaper, including 10% post-consumer waste.